Massive binary black holes from Population II and III stars

Guglielmo Costa
guglielmo.costa@univ-lyon1.fr

Main collaborators:
PARSEC Team → Bressan A., Shepherd K.G., Volpato G. et al.
http://stev.oapd.inaf.it/PARSEC

DEMOBLACK Team → Iorio G., Mapelli M., Santoliquido F., et al.
http://demoblack.com

http://demoblack.com/

POPSYCLE
Project

Outline

- New stellar tracks
- Comparison between Pop. III and Pop. II
- Binary evolution of Pop. III stars

  Costa et al. 2023 (submitted)

New PARSEC tracks

Details

PARSEC v1.0 – v1.2
(Bressan et al. 2012; Chen et al. 2014; Fu et al. 2018)

PARSEC v2.0
(online database at http://stev.oapd.inaf.it/PARSEC)
(Costa et al. 2019a,b; Costa et al. 2021; Nguyen et al. 2022)

- Diffusive approach to treat mixing and chemical evolution at the same time (Marigo et al. 2013);
- Rotation: main effects on geometry, mixing, Ang. Mom. transport and mass loss enhancement;

- Winds for WR stars (Sander et al. 2019);
- EOS, now including the pair-creation process (Timmes&Arnett, 1999);
- Nuclear reaction network (72 reactions with 33 isotopic elements);

- Computation and release of new sets of low- and intermediate-mass tracks with rotation;
- New isochrones with rotation;
- Database publicly accessible:
  - Masses 0.09 – 14 $M_{\odot}$
  - $Z = [0.004 – 0.017]$
  - $\omega = [0.0 – 0.99]$

(ω = ang. vel. / ang. vel.^{3} crit.)

New PARSEC tracks

in one slide

88 Tracks per set
× 15 Metallicities (Z)
~ 1300 new tracks

From 2 $M_\odot$ to 600 $M_\odot$
Complete up to:

- E-AGB phase
- O-burning phase
- Pulsating instability (PI) regime

Population III	Population II	Population I
$0 \leq Z \leq 10^{-6}$	$10^{-5} – 10^{-4} < Z \leq 10^{-2}$	$Z > 10^{-2}$

(Costa, Sheperd et al., in prep.)

New PARSEC tracks

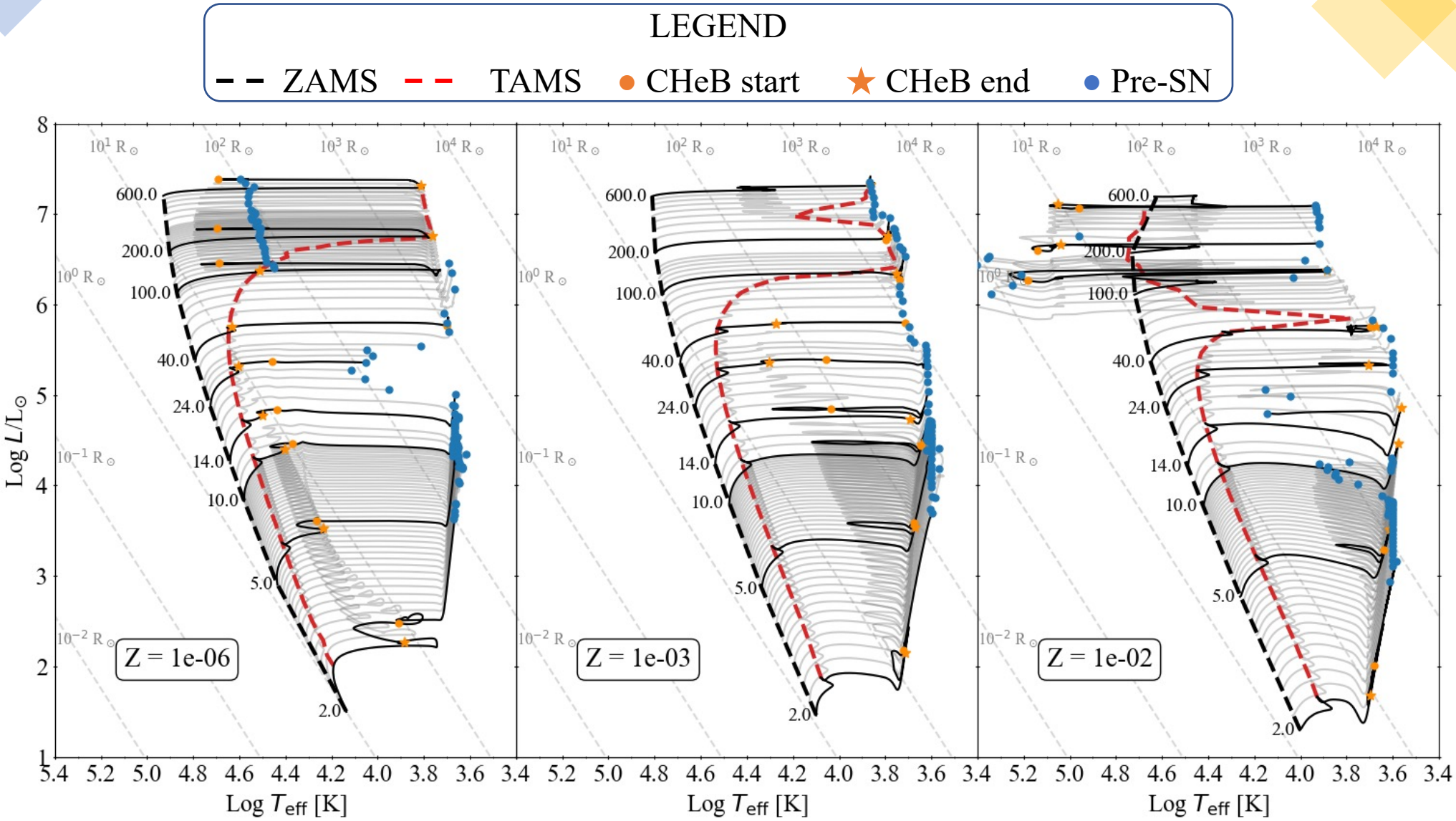

(Costa, Sheperd et al., in prep.)

Final Masses at different metallicity

Project with Kendall
G. Sheppard
(SISSA PhD student)

LEGEND

$M_{initial}$ M_{final} $M_{He\text{-}Core}$ $M_{CO\text{-}Core}$

Fate: ● BH ★ PPISN ✕ PISN

Limits from
Heger & Woosley 2002

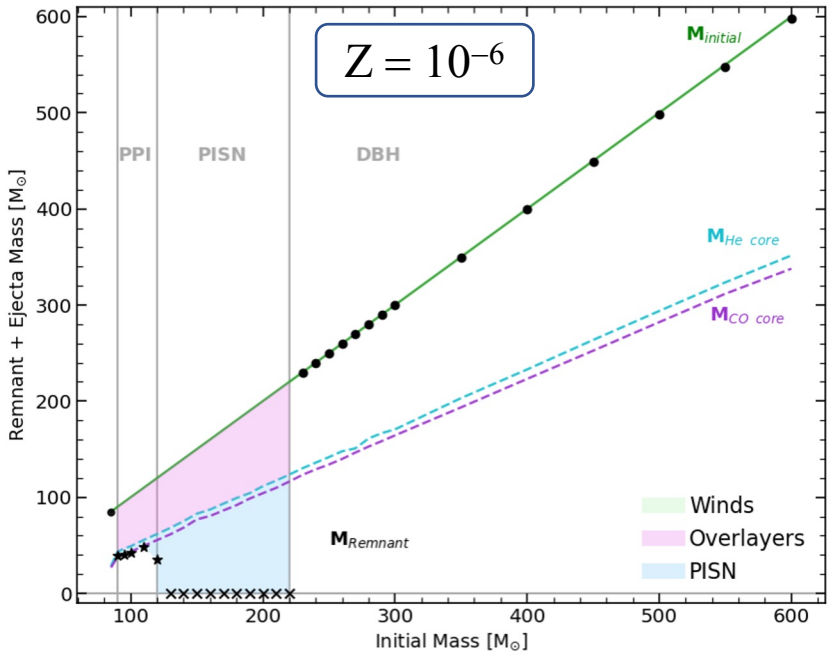

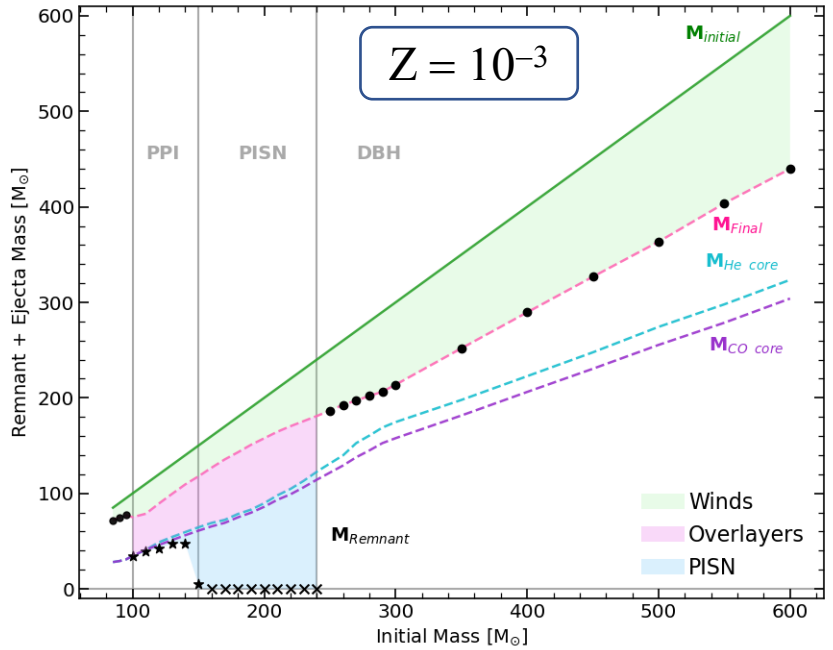

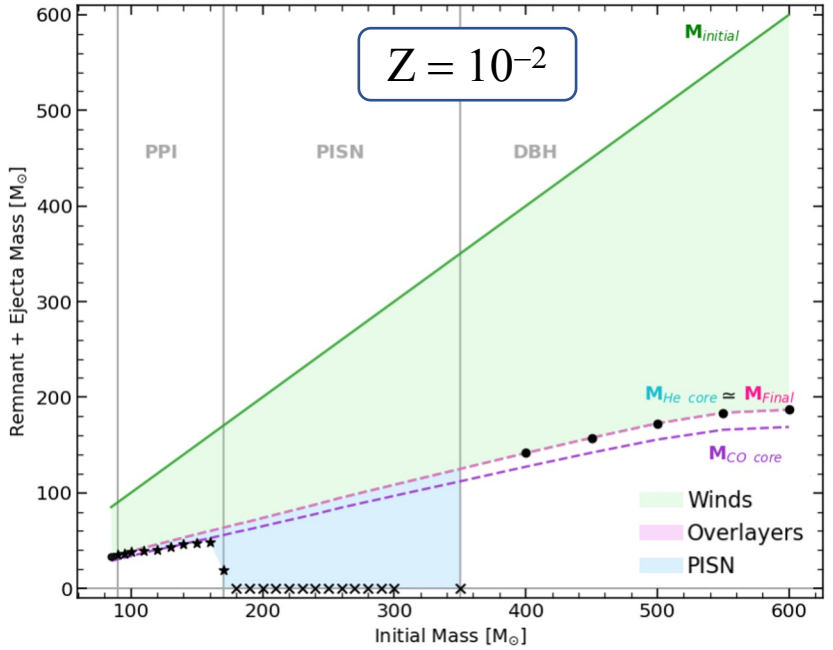

(Costa, Sheperd et al., in prep.)

Total yields at different metallicity

Project with Kendall G. Sheppard (SISSA PhD student)

Stellar Yields for massive stars:
We use Heger & Woosley 2002 results from hydrodynamic simulations of the PPI explosion and use the He-core masses at the end of evolution as a proxy for the final explosion.

$Z = 10^{-6}$

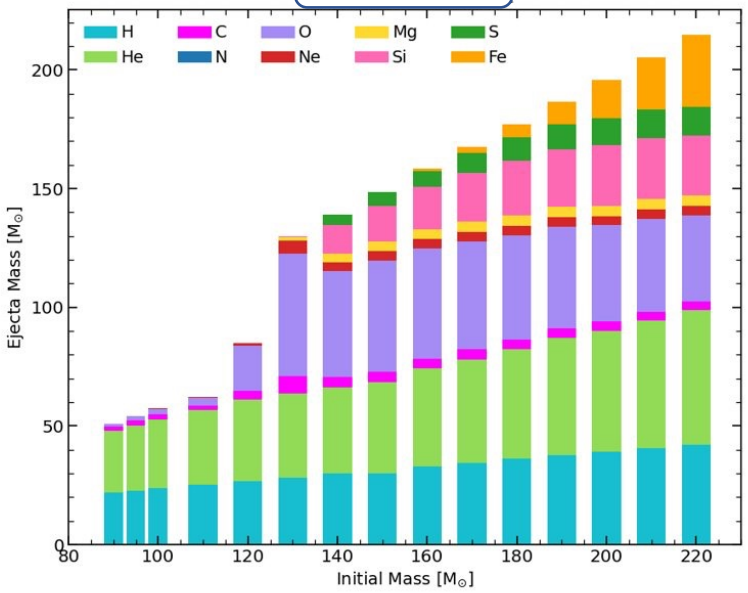

$Z = 10^{-3}$

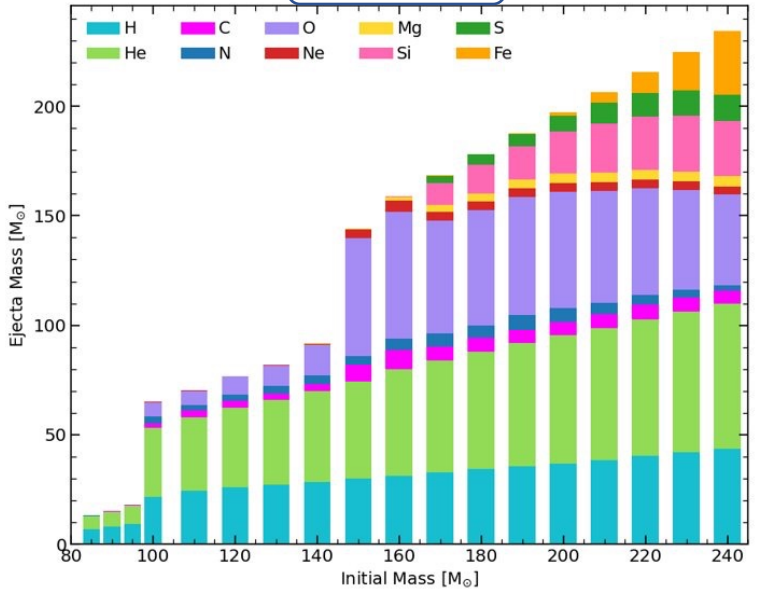

$Z = 10^{-2}$

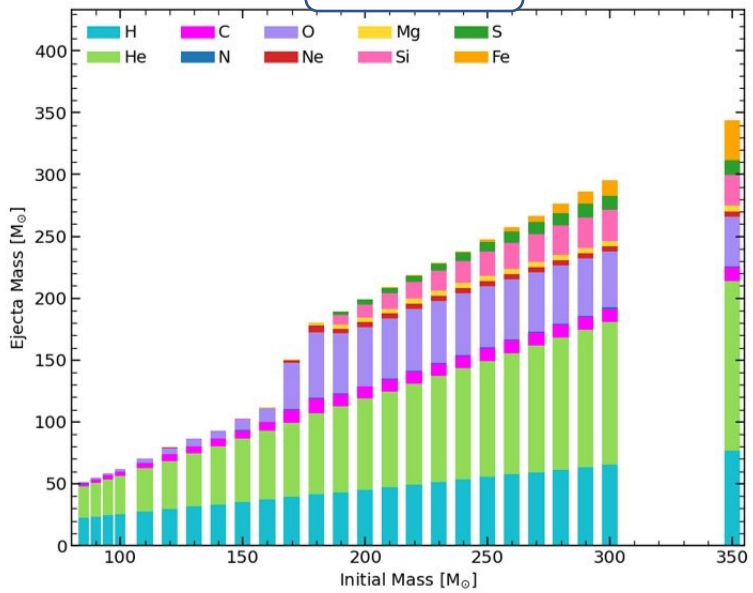

(Costa, Sheperd et al., in prep.)

Effects of pulsation mass loss in very massive Pop. III stars

See talk by Guglielmo Volpato

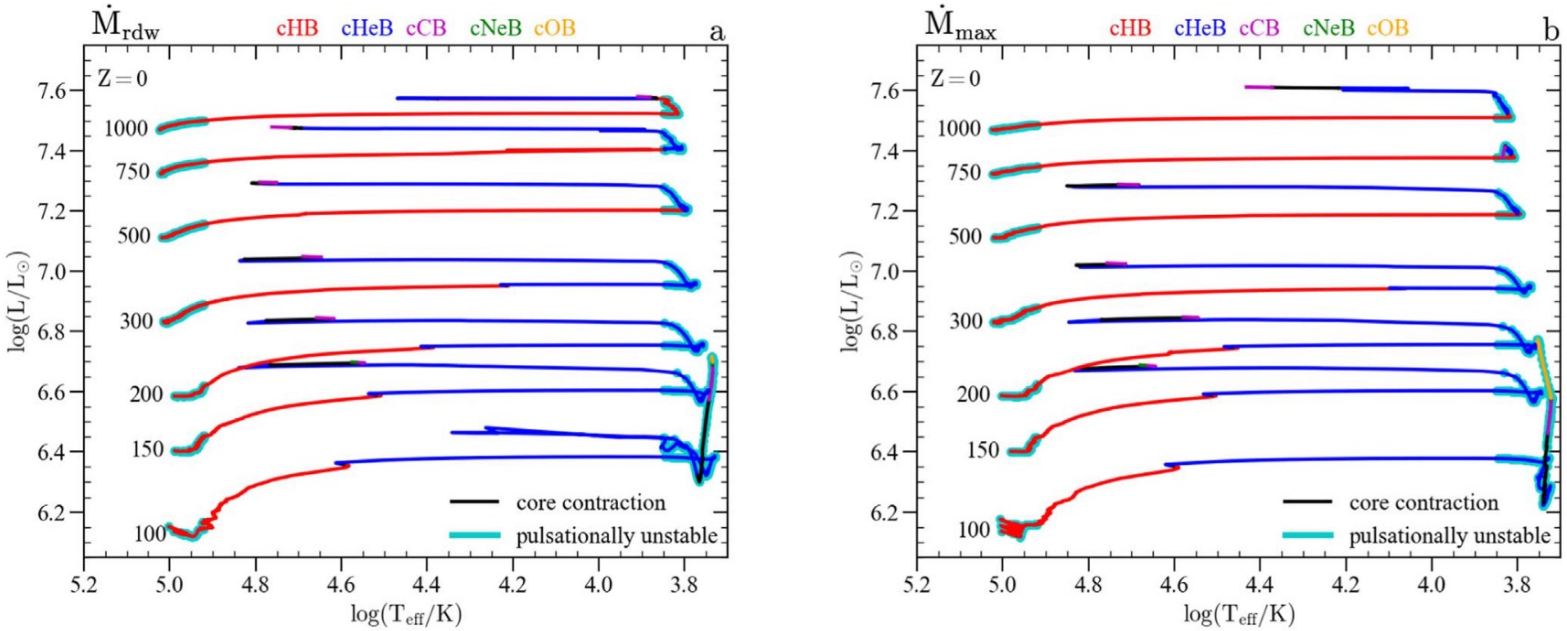

Volpato et al. 2023

Outline

- New stellar tracks
- Comparison between Pop. III and Pop. II
- Binary evolution of Pop. III stars

  Costa et al. 2023 (submitted)

Pop. III vs. Pop. II

HR diagram

Pop. III stars typical properties (Cassisi & Castellani 1993; Marigo+2001; Murphy+2021):

- **IMF not well constrained!** (see Klessen & Glover 2023)
- They are hotter and more compact than Pop. II stars.
- Almost no winds!

- They cannot ignite the CNO tri-cycle near the ZAMS;
- They reach high temperatures at their center during MS;
- Triple-*a* reaction (He-Burning), even in the MS;
- Smoother transition to the CHeB phase.

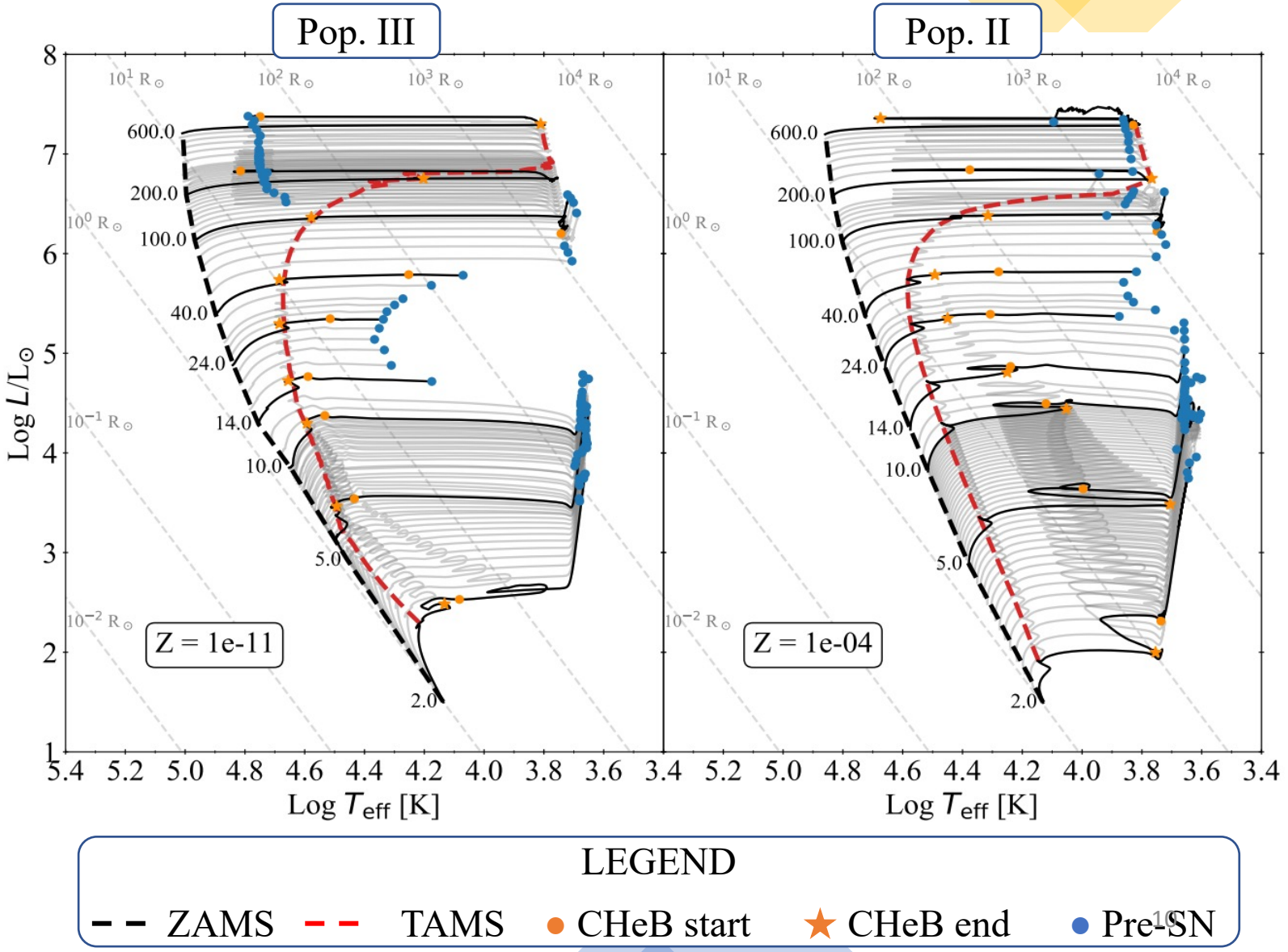

Pop. III vs. Pop. II

Radius evolution

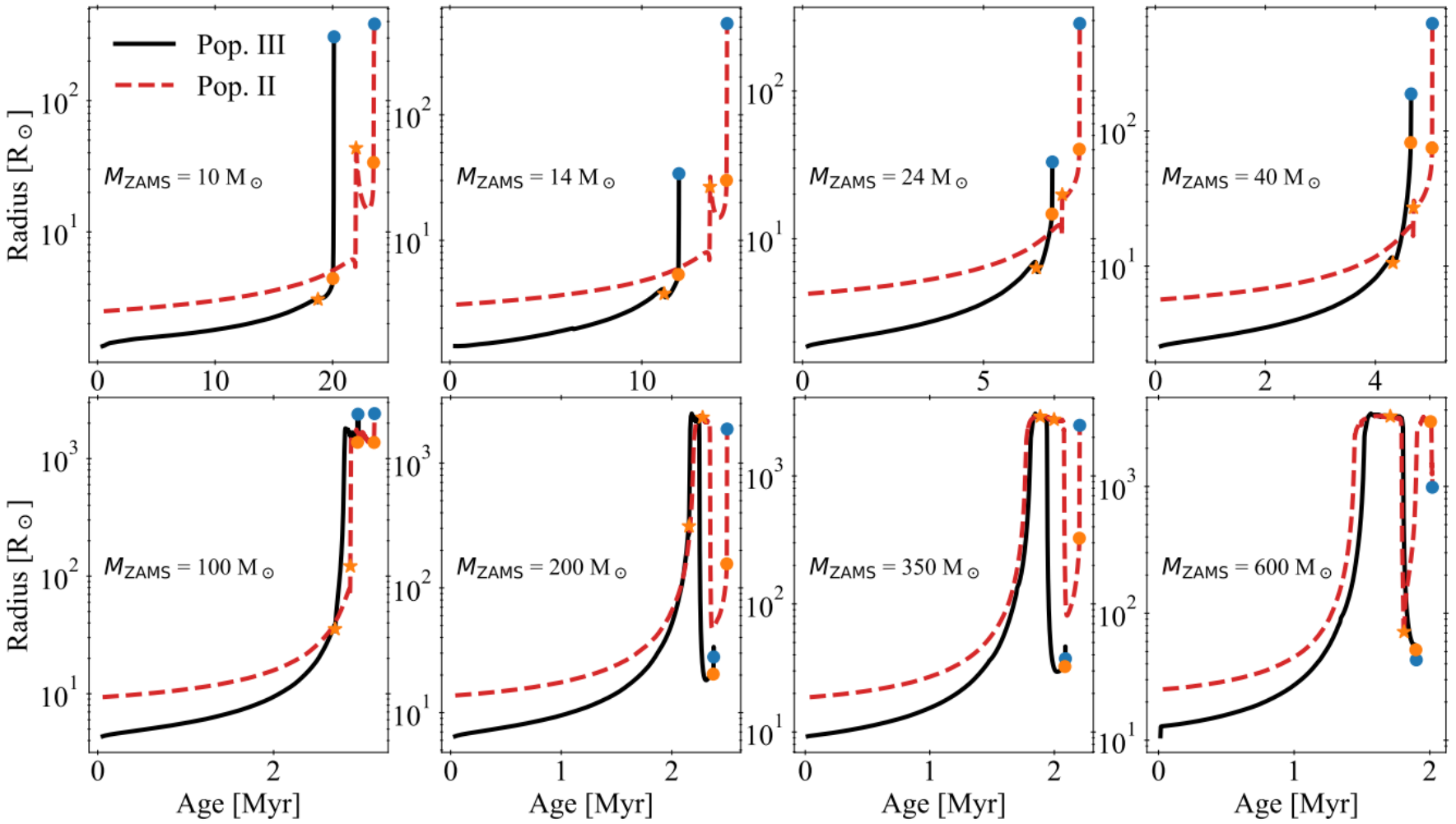

Masses in the stellar graveyard

Pop. III stars are the main candidates as possible progenitors of the most massive BBHs observed by the LIGO–Virgo–KAGRA (LVK) collaboration (Abbott et al. 2020a,b, 2021a,b).

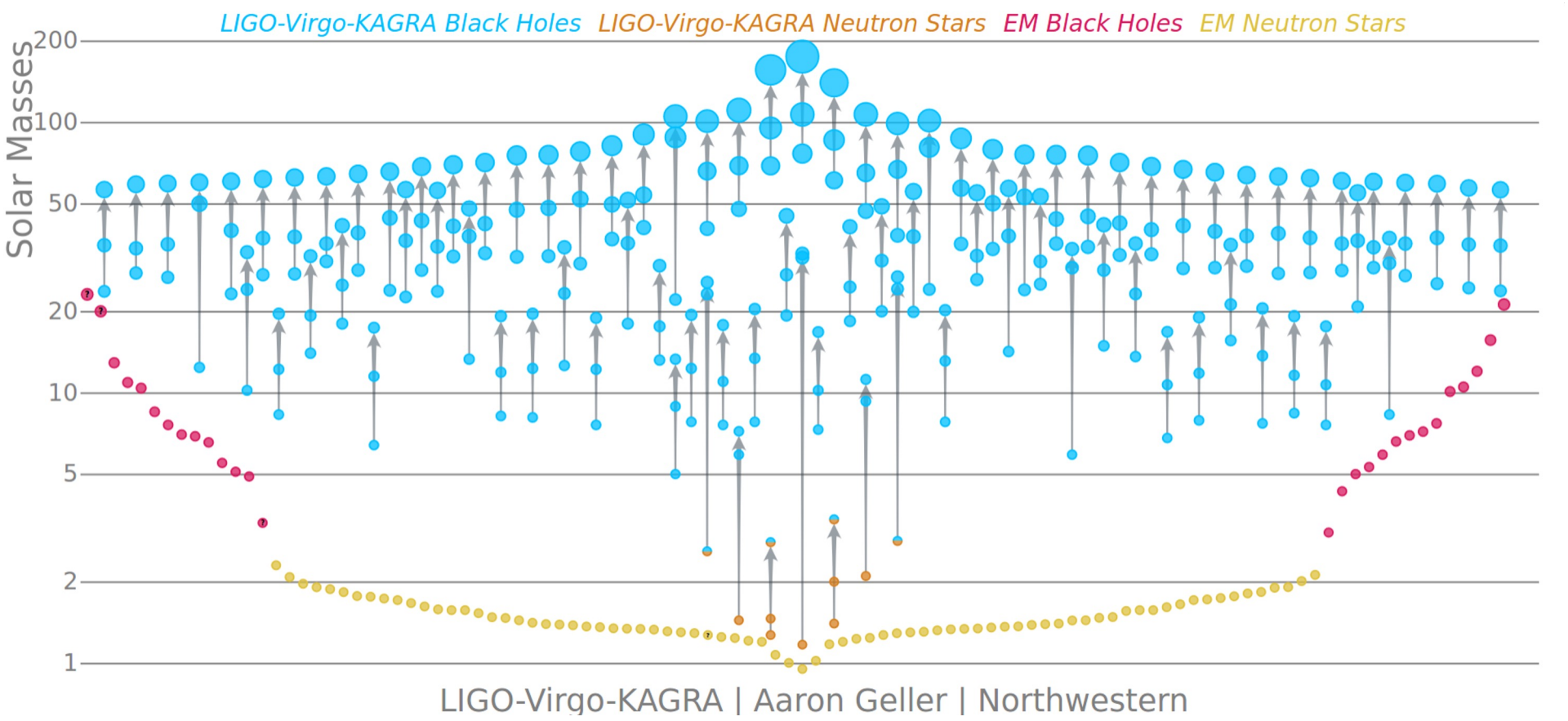

https://ligo.northwestern.edu/media/mass-plot/index.html

Masses in the stellar graveyard

Pop. III stars are the main candidates as possible progenitors of the most massive BBHs observed by the LIGO–Virgo–KAGRA (LVK) collaboration (Abbott et al. 2020a,b, 2021a,b).

PI mass gap edges (Woosley 2017): 60 – 130 $M_\odot$

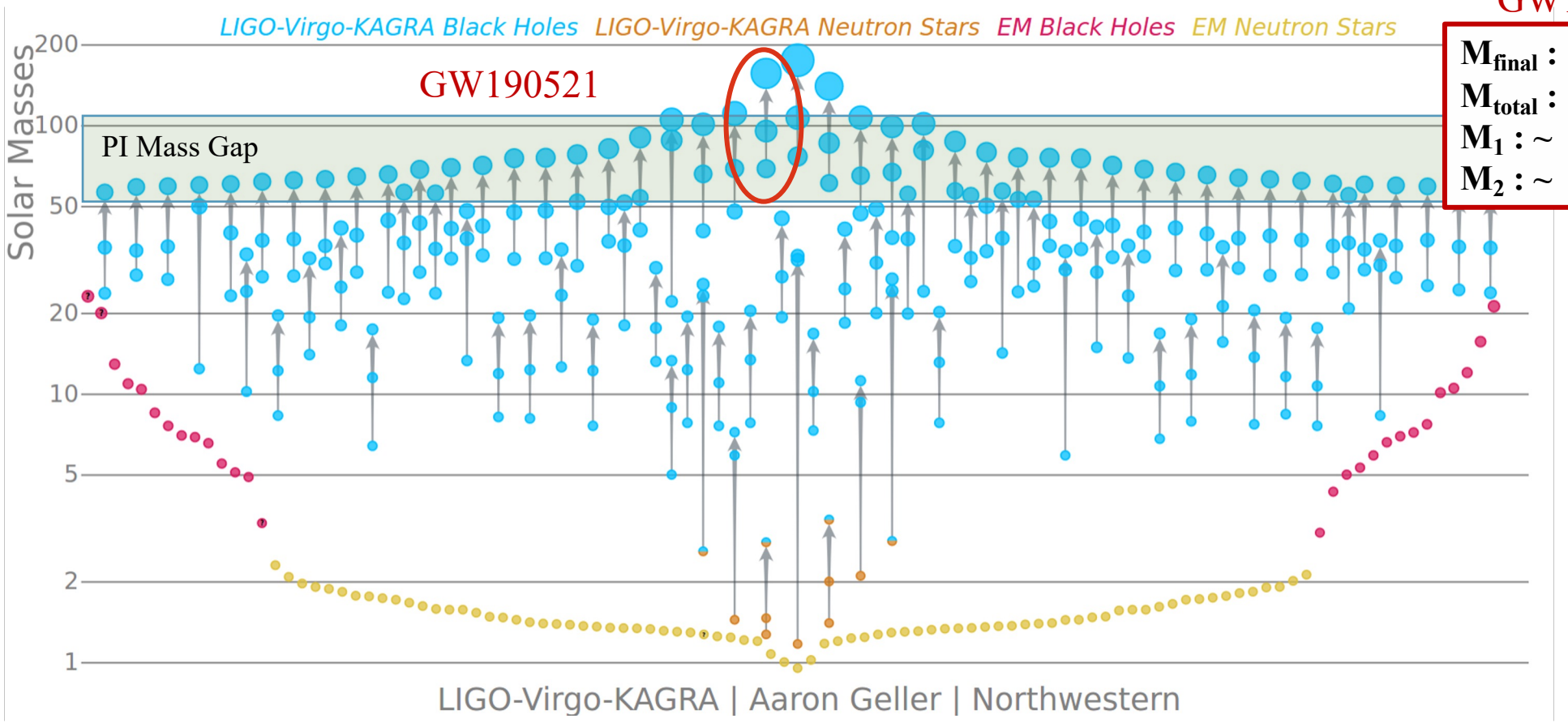

GW190521

M_{final} : 156.3 $M_\odot$
M_{total} : 163.9 $M_\odot$
M_1 : ~ 90 $M_\odot$
M_2 : ~ 70 $M_\odot$

https://ligo.northwestern.edu/media/mass-plot/index.html

Outline

- New stellar tracks
- Comparison between Pop. III and Pop. II
- Binary evolution of Pop. III (and Pop. II) stars

Costa et al. 2023 (submitted)

Population synthesis
SEVN

https://gitlab.com/sevncodes/sevn

SEVN v2 (Iorio et al. 2022) follows the evolution of stellar properties by interpolating a set of stellar tracks and models the main binary evolution processes with a semi-analytic formalism.

BHs mass spectrum of single stellar populations

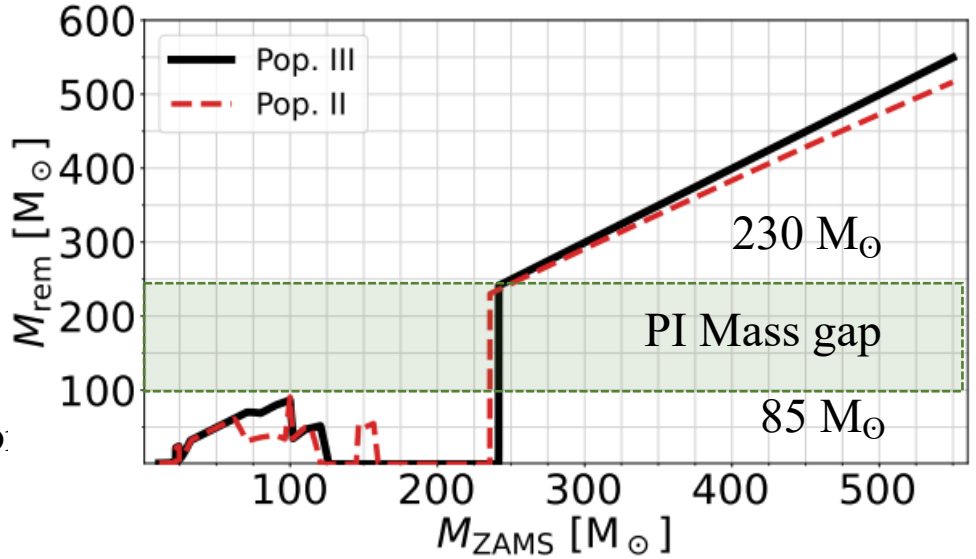

SEVN can evolve populations of **single stars** and **binaries**.

- Rapid (parallel with open MP)
- Flexible (modular, object-oriented, tracks tables)
- Follows the evolution of stars from PMS to compact objects (CO) formatio
- Treats the main binary processes (MT, RLO, CE, Tides, etc..)

Input
Binaries list
IMF, *q*, *P*, and *e*

→

Outputs
Catalogs of COs populations.

Population synthesis

Initial conditions

4 **IMF**:

- **LOG**, Logflat, Stacy & Bromm 2013;
- **LAR**, Larson et al., 1998;
- **TOP**, Top-heavy, Liu-Bromm et al. 2020;
- **KRO**, Kroupa 2001;

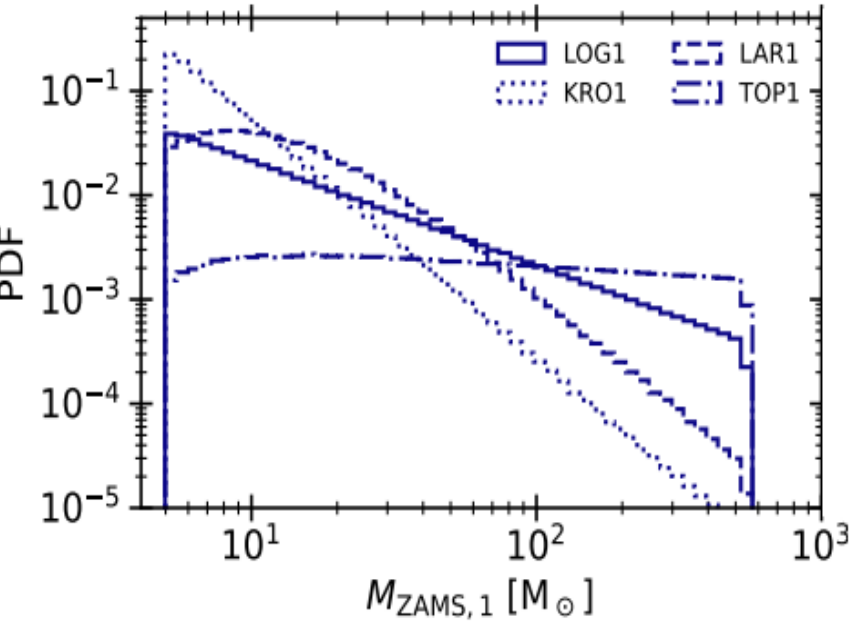

3 **Mass ratios**, q:

- **S12**, Sana et al. 2012;
- **SB13**, Stacy & Bromm 2013;
- **Sorted** distribution;

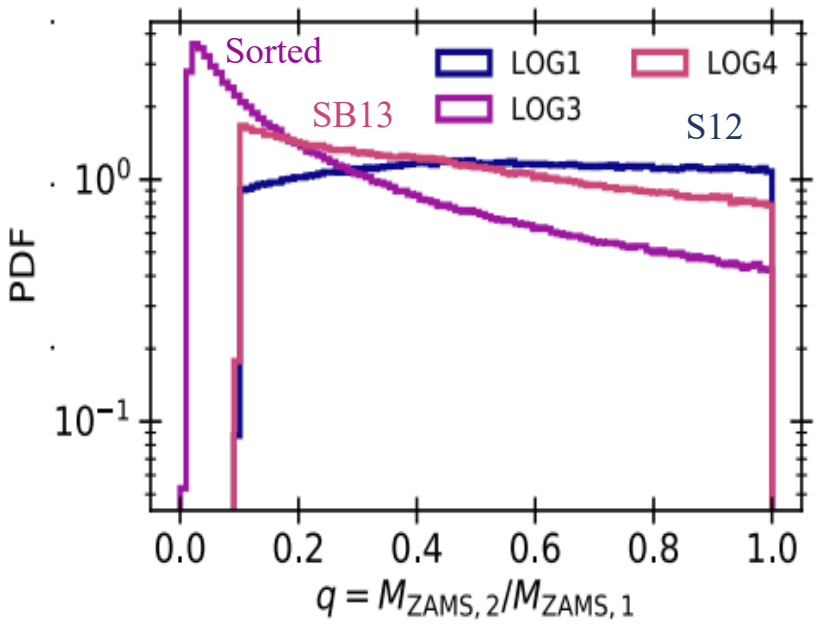

2 **Orbital periods, *P*:**

- **S12, Sana** et al. 2012 **(SHORT)**;
- **SB13**, Stacy & Bromm 2013 **(LONG)**;

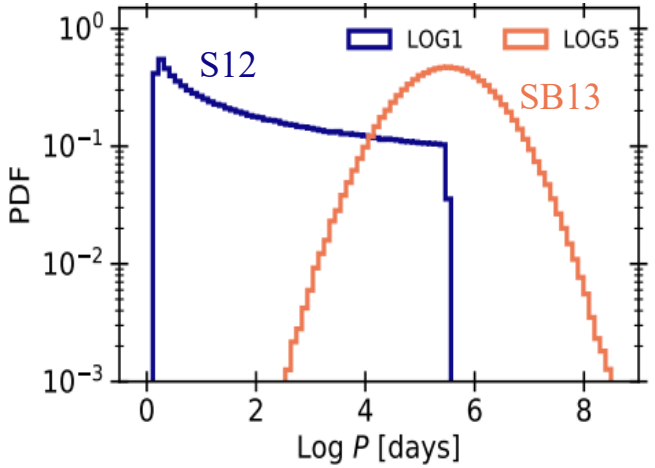

2 **Eccentricity** distribution, e:

- **S12**, Sana et al. 2012;
- **Thermal** distribution, Kinugawa et al. 2014.

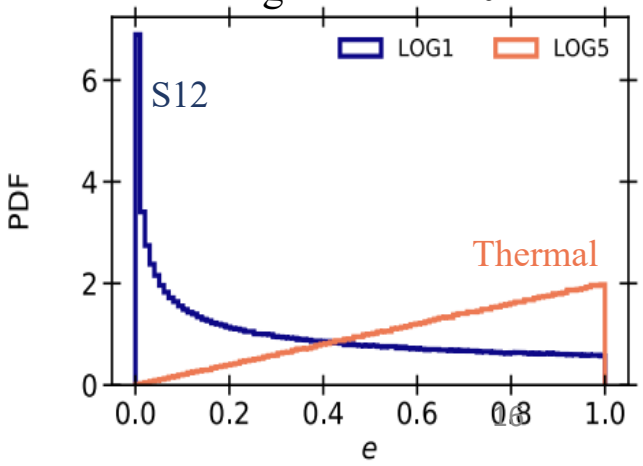

Population synthesis

Initial conditions

IC for the binary population of Pop. III and Pop. II stars.

11 combinations of the four initial properties by varying distributions of the **IMF, *q*, *P*, and *e*.**

$M_{ZAMS,1} = [\,5 - 550]\ M_\odot$

$M_{ZAMS,2} \geq 2.2\ M_\odot$

We set the total number of generated binaries to obtain **10^7 binaries** in the high-mass regime. $M_{ZAMS,1} \geq 10\ M_\odot$ and $M_{ZAMS,2} \geq 10\ M_\odot$ by construction.

~ 220 Milions binaries

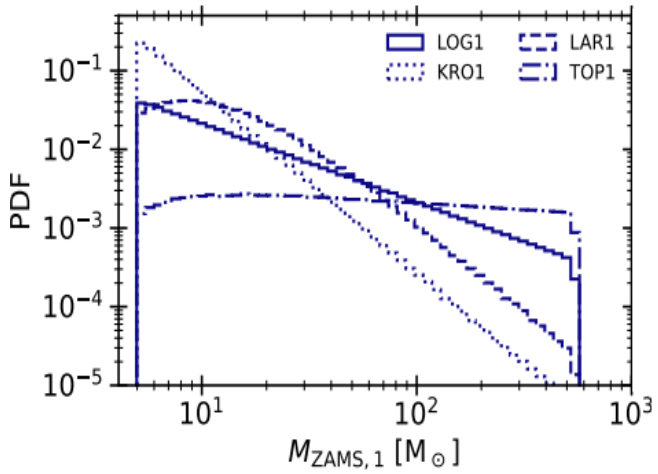

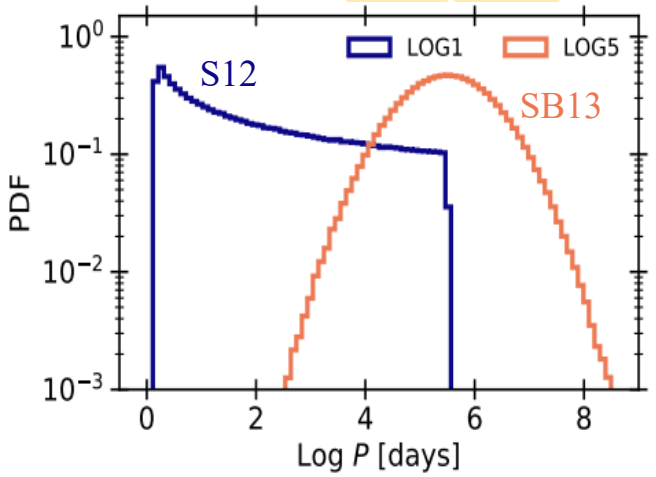

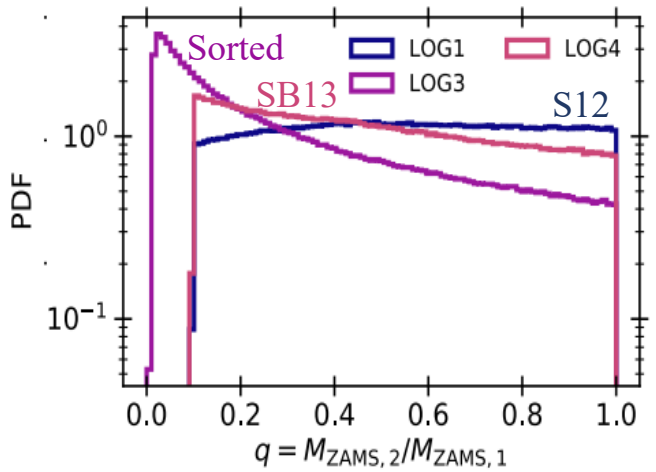

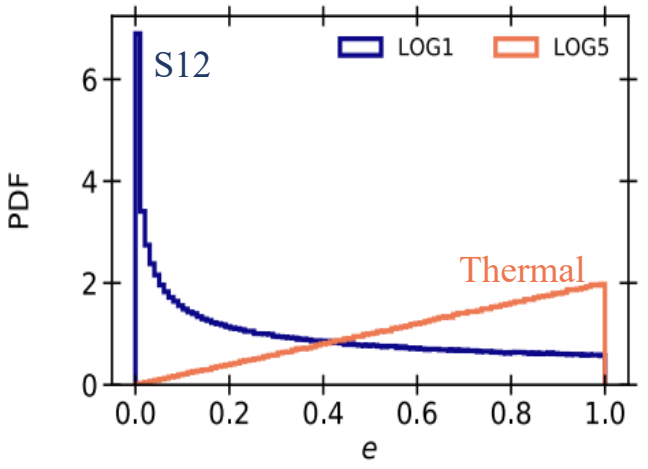

Population synthesis

Results

Configuration	Mass ratio	Period	Eccentricity
1	S12	S12 (short)	S12
5	SB13	SB13 (long)	Thermal

BBHs which merge within a Hubble time (~ 14 Gyr), BBHm

BBHm (%)	LOG1	LOG5	KRO1	KRO5	LAR1	LAR5	TOP1	TOP5
Pop. III	11.25	0.68	14.66	0.85	14.34	0.91	6.47	0.36
Pop. II	13.53	0.86	16.23	1.15	16.15	1.16	8.52	0.48

The numbers of BBHs born from Pop. III stars are similar to those of BBHs born from Pop. II stars for all the considered models.

Population synthesis

Results

The masses distribution of Pop. III and Pop. II BBHms are similar.

- **A few BBHm with one component above the pair-instability mass gap (0.1 – 3 %).** Assuming that PI Mgap spans from 85 to 230 $M_{\odot}$, we find that BBH mergers with primary BH masses above the gap are up to 3.3 % (LOG3, Pop. III) and up to 0.09% (TOP5, Pop. II).
- **BBHm inside the gap are rare (< 2.5 %).** BBHms with primary BH mass inside the gap are up to 1.9% (LOG3, Pop. III) and up to 2.4% (TOP5, Pop. II).
- **$M_s < 45\ M_{\odot}$** for both Pop. II and III stars.
- **Pop. II stars produce more BBHms with primary BH mass above the gap than Pop. III.**

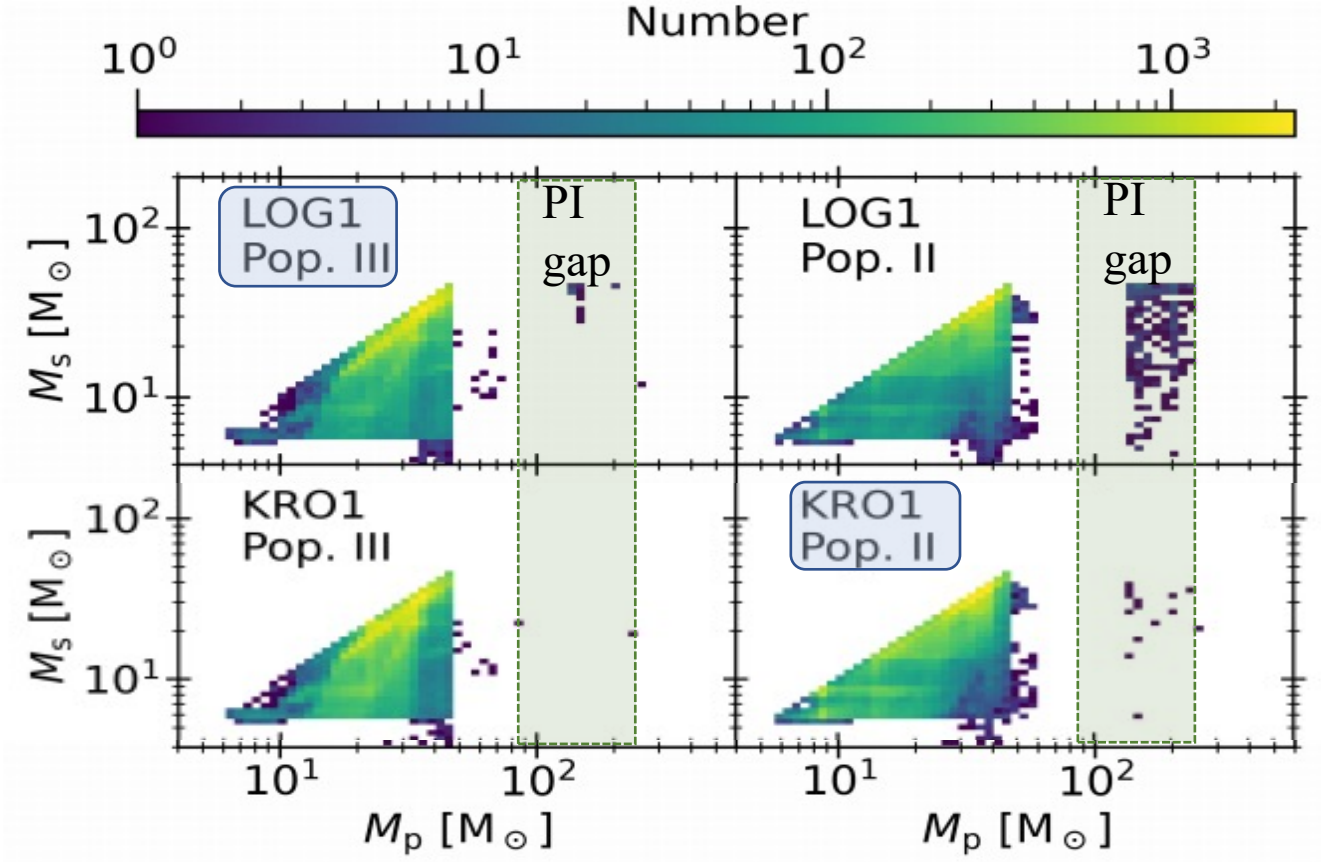

Population synthesis

Results

The masses distribution of Pop. III and Pop. II BBHms are similar.

- **The most common primary BH masses are around 30 – 40 $M_\odot$.**
- There is a **dearth of low-mass primary BHs (8 – 10 $M_\odot$)** with respect to LVK mergers (Abbott et al. 2019, 2021d,c) in all of our runs. Due to the negligible mass loss rate and compact stellar radii.
- **The most common secondary BH mass for Pop. III stars is 20 $M_\odot$**, while for Pop. II stars it is model dependent.

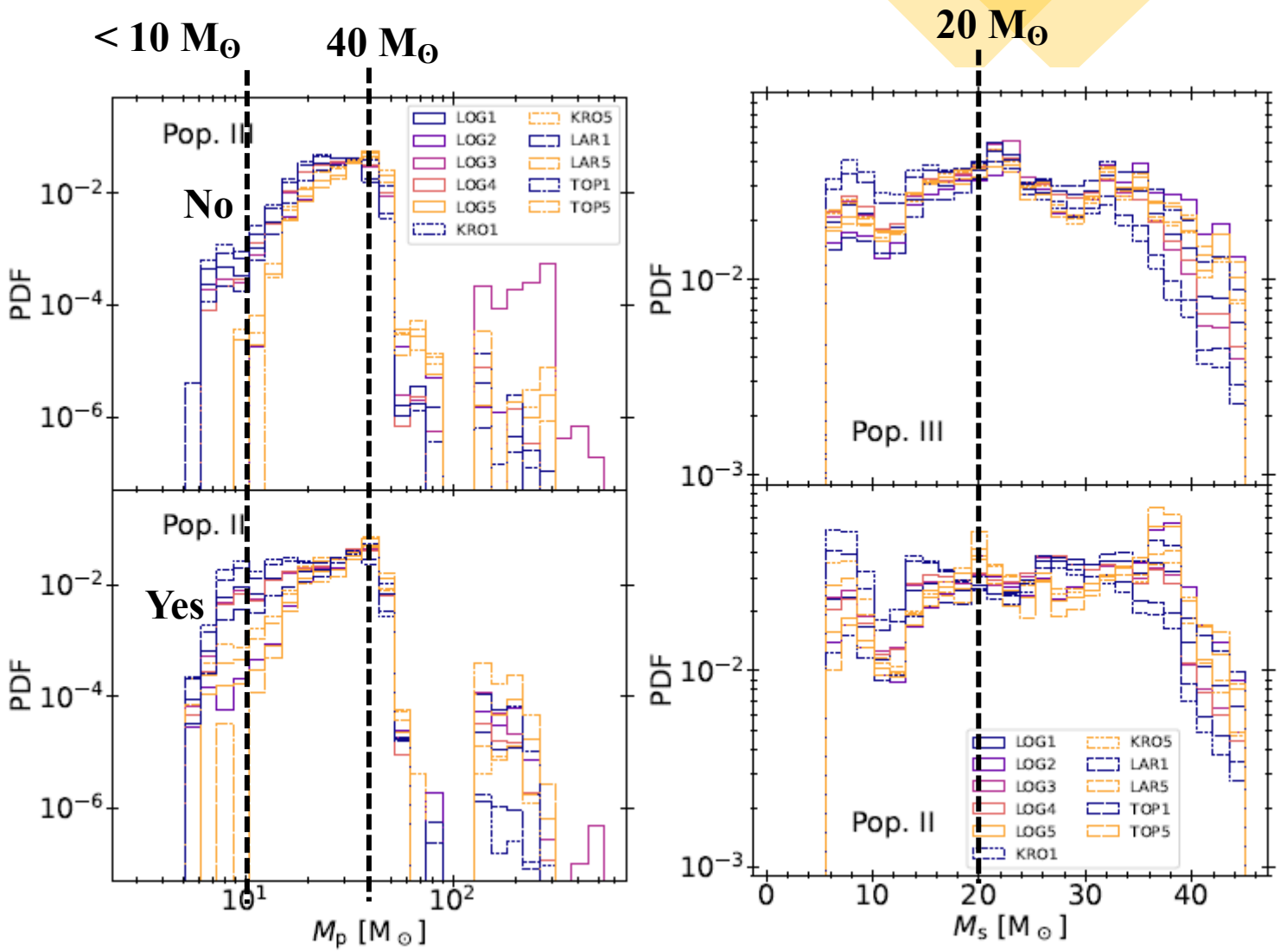

Results – Formation channels

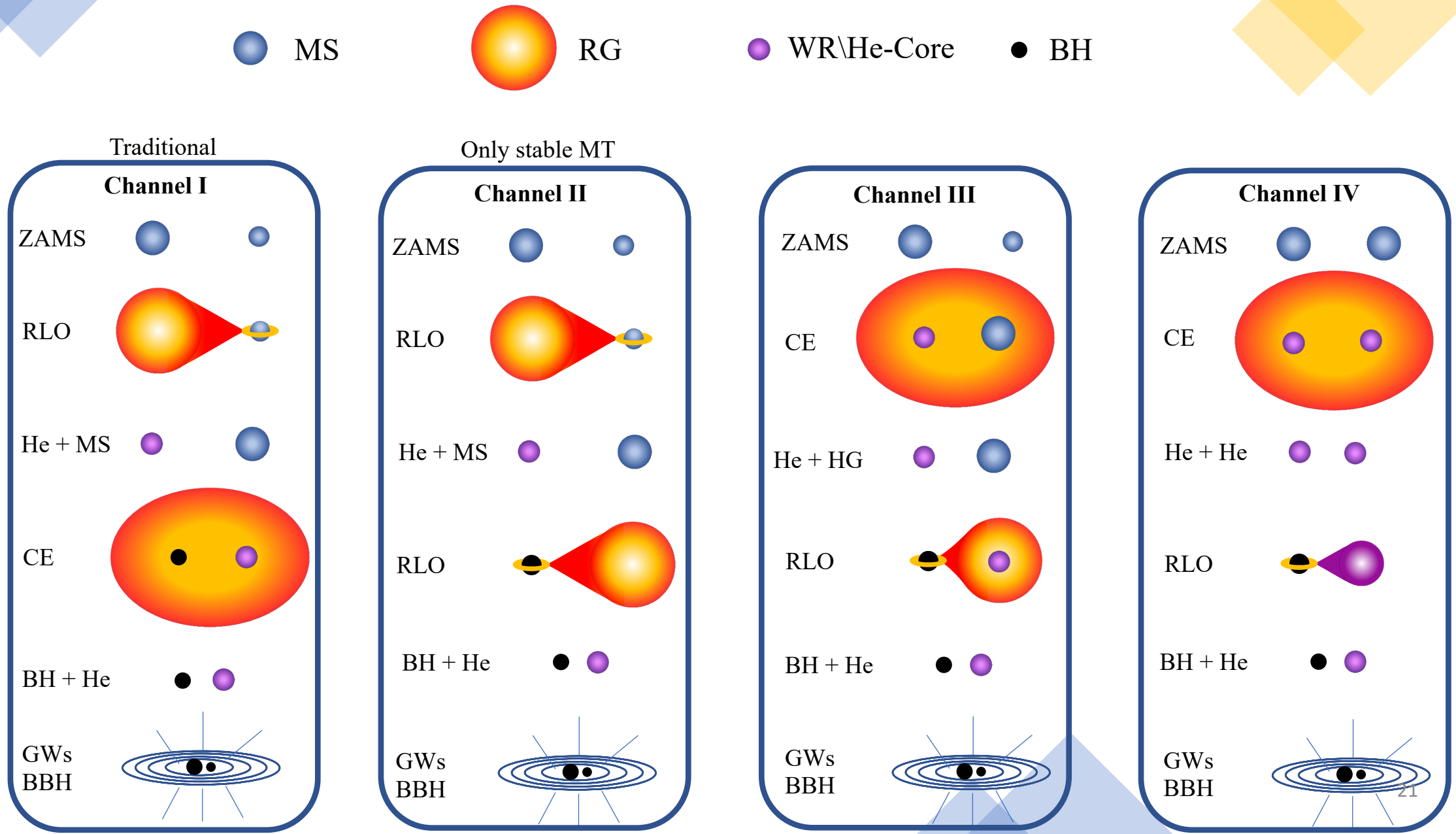

Results – Formation channels

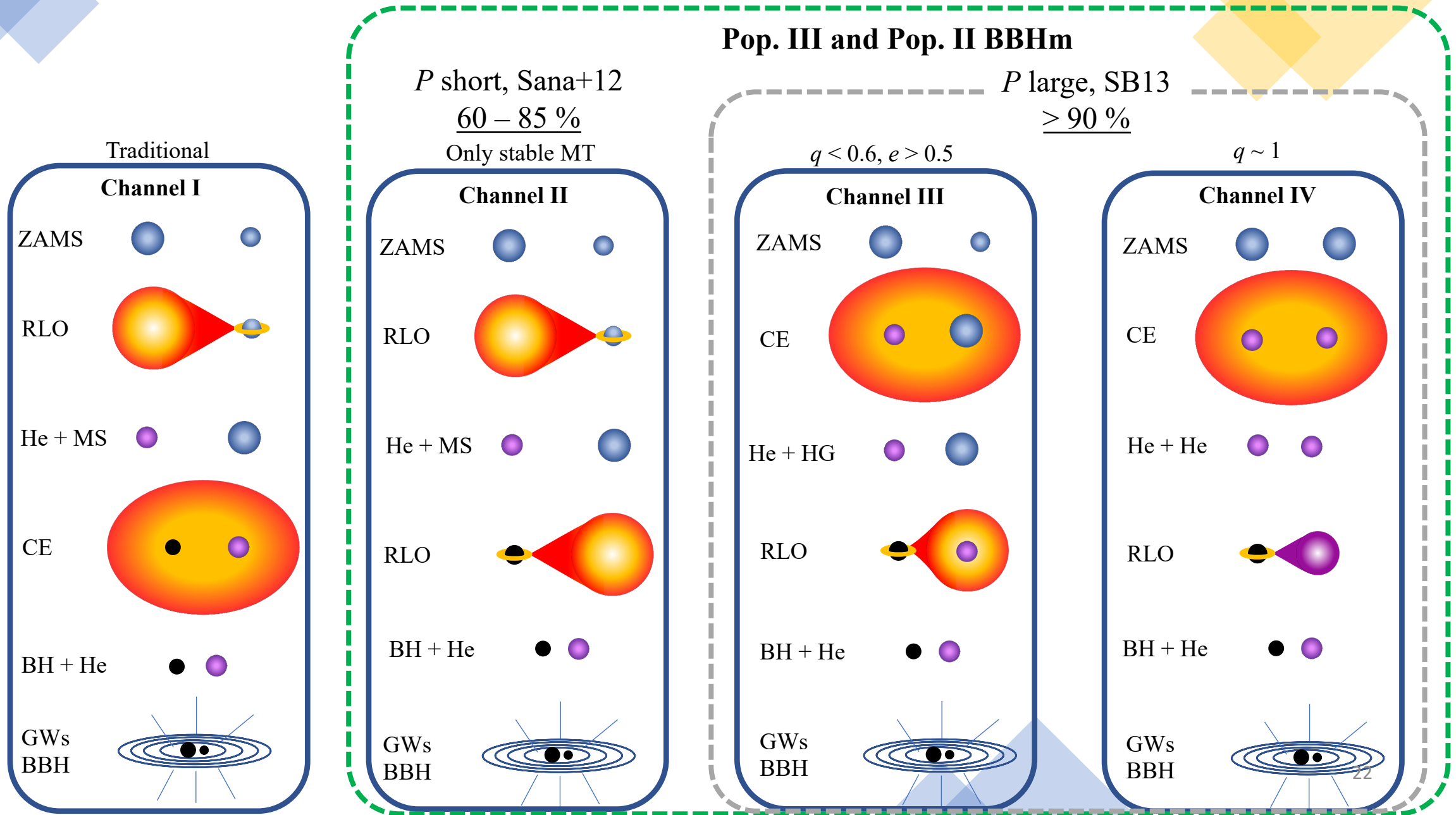

Results – Formation channels

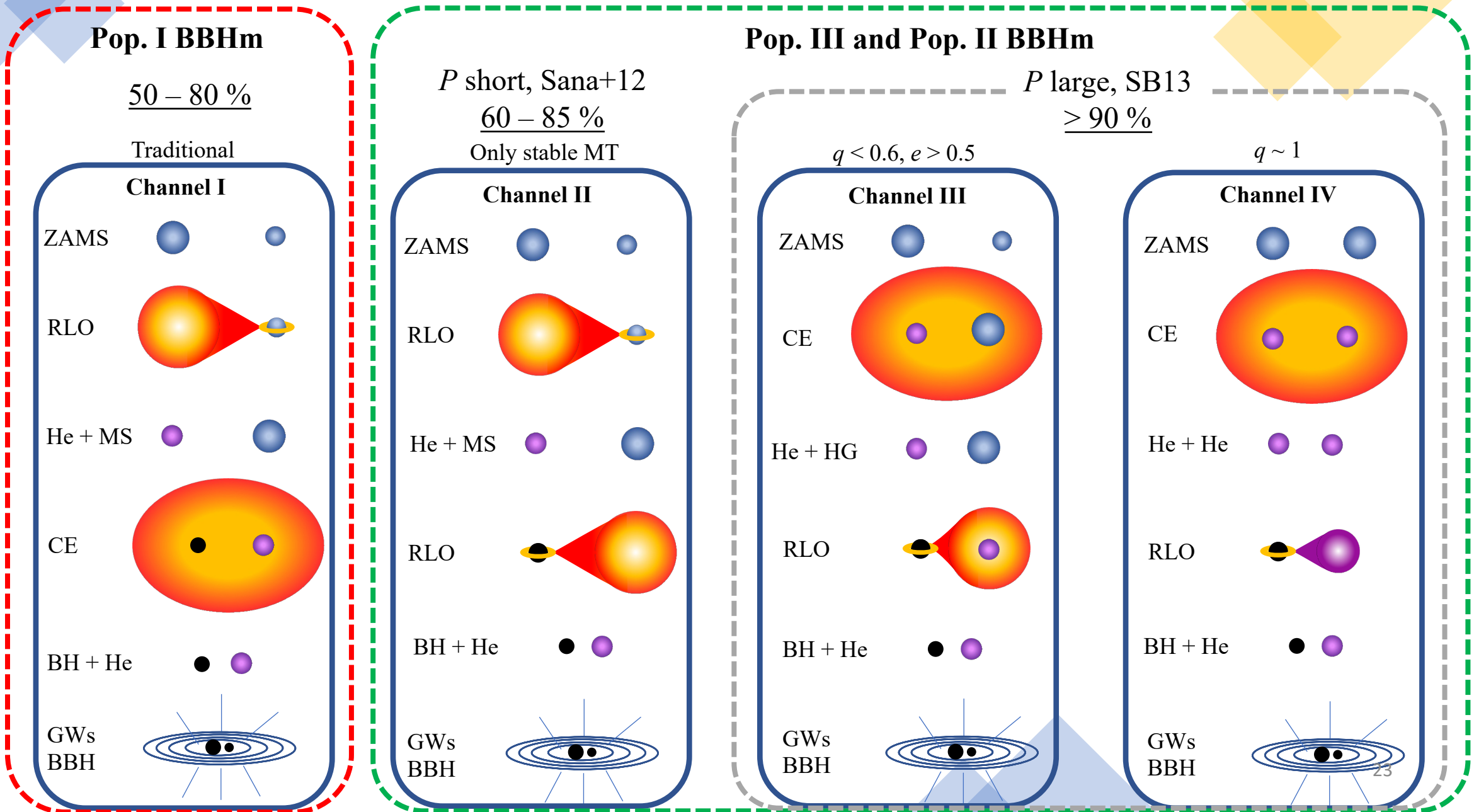

Conclusions

- We have presented a new set of tracks obtained with the stellar evolution code parsec, soon publicly available at http://stev.oapd.inaf.it/PARSEC.

- Massive Pop. III stars ($M_{ZAMS} > 100\ M_{\odot}$) end their life as BSG stars, while Pop. II stars die as YSG or RSG stars.

- **Pop. III and II stars produce a similar BBHs populations (**Costa et al. 2023, submitted)

- Most BBH mergers from both Pop. II and Pop. III stars have primary BH mass below the mass gap.

- We find no mergers with secondary BH mass above the gap.

- The vast majority (60 – 80 %) of Pop. III and II BBHm progenitors evolve via channel II in our fiducial model. In contrast, Pop. I binaries evolve via channel I (50 – 80 % BBH mergers, Iorio et al. 2022).

Thanks

Backup-Slides

The ZAMS mass range we consider in this work is comparable to the one explored by Tanikawa et al. (2021b). Discrepancies between our single star evolution models. The very massive stars ($M_{ZAMS} > 200\ M_\odot$) considered by Tanikawa et al. (2021b) end the MS as compact blue super-giant stars, while our very massive stars expand during the MS and become RSG stars already at the end of the MS.

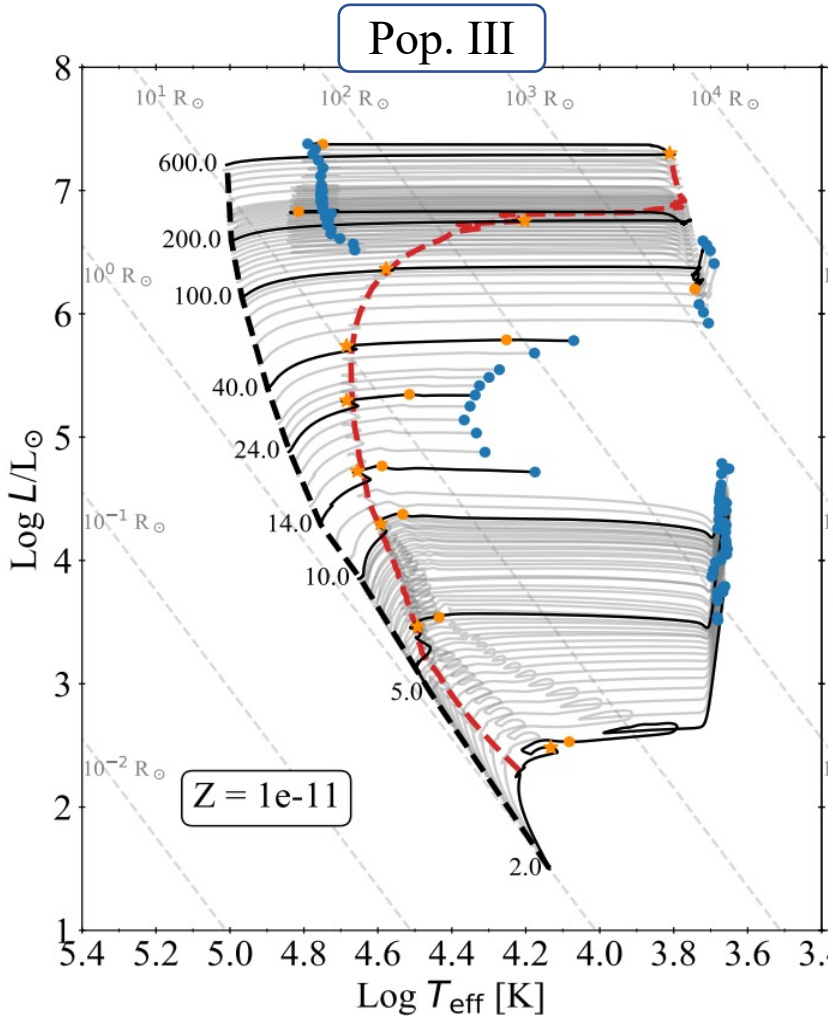

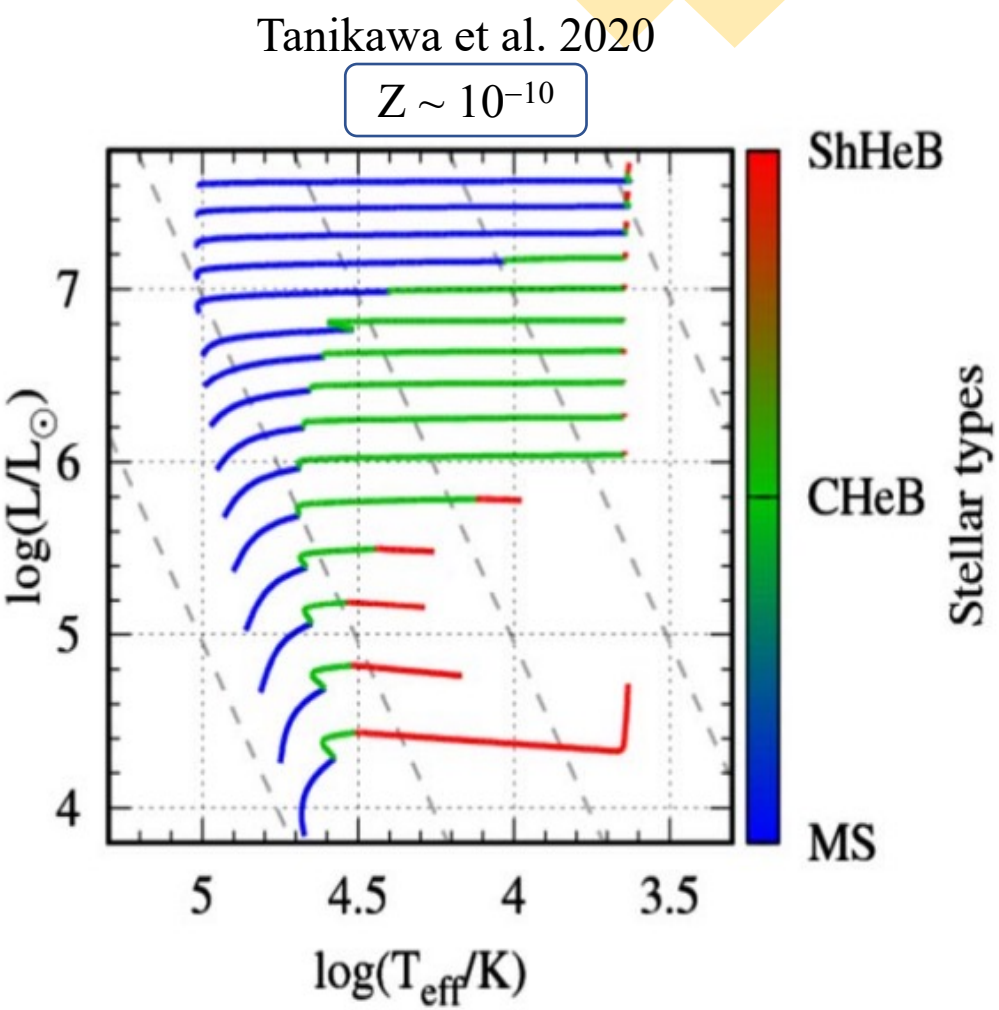

In our models, we do not have any mergers with both BHs above the mass gap, while these are very common in their fiducial model. This is due to the differences of stellar models, the very massive binary systems by Tanikawa et al. (2021b) undergo stable mass transfer and leave BHs above the mass gap, while our very massive binary systems start an unstable common envelope phase as soon as they leave the MS and merge prematurely, before becoming BHs.

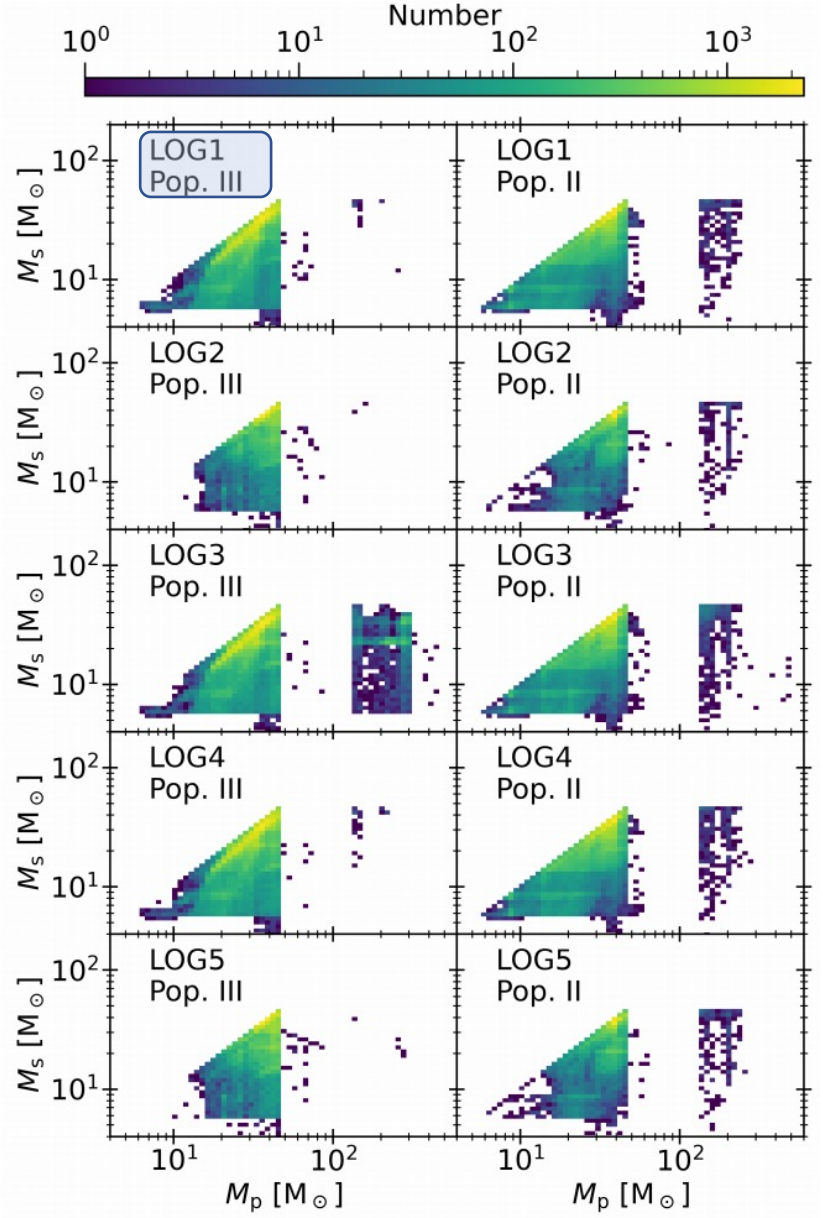

Tanikawa et al. 2020

$Z \sim 10^{-10}$

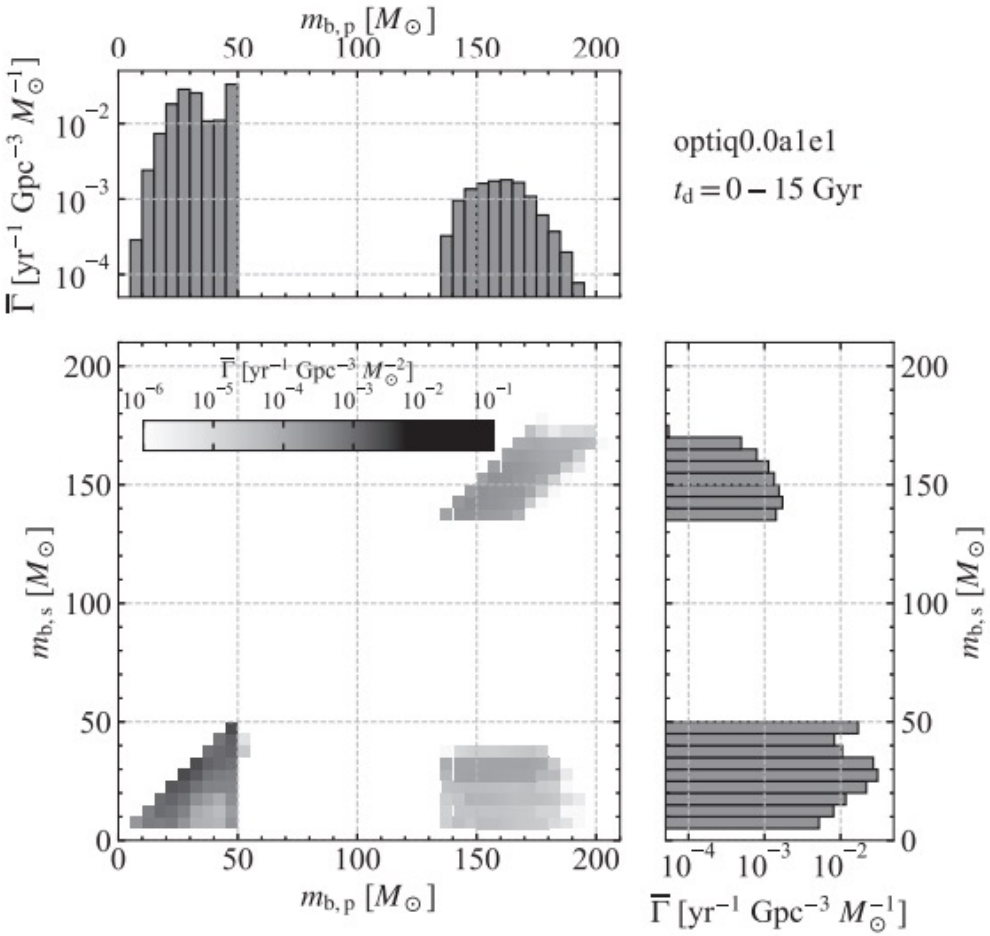

Population synthesis
SEVN - setup

https://gitlab.com/sevncodes/sevn

FINAL PHASES

We use the rapid supernova model by Fryer et al. (2012), but we draw the NS masses from a Gaussian distribution centred at $M = 1.33\ M_{\odot}$.

We take into account the pair instability and pulsation pair instability using the model by Mapelli et al. (2020), obtained from Woosley, 2017.

We use the model KGM20 by Giacobbo & Mapelli (2020) to draw the natal kicks.

$$V_{\rm kick} = f_{\rm H05}\,\frac{\langle M_{\rm NS}\rangle}{M_{\rm rem}}\,\frac{M_{\rm ej}}{\langle M_{\rm ej}\rangle},$$

MASS TRANSFER

We adopt a stable mass transfer for MS and HG donor stars (during RLO), while we follow the Hurley et al. (2002) prescriptions in all the other cases.
At the onset of RLO, we circularise the orbit at periastron.

We set the default RLO mass accretion efficiency to $f_{\rm MT} = 0.5$, and assume that the mass not accreted during the RLO is lost from the vicinity of the accretor as an isotropic wind.

$$\dot{M}_{\rm a} = \begin{cases} \min\left(\dot{M}_{\rm Edd},\ -f_{\rm MT}\,\dot{M}_{\rm d}\right) & \text{if the accretor is a compact object,} \\ -f_{\rm MT}\,\dot{M}_{\rm d} & \text{otherwise,} \end{cases}$$

During CE, we assume an efficiency parameter $\alpha_{\rm CE} = 1$ and estimate the envelope binding energy using the same $\lambda_{\rm CE}$ formalism as in Claeys et al. 2014.

Population synthesis

Initial conditions

IC for the binary population of Pop. III and Pop. II stars.

4 different IMF:

- **LOG**, Logflat, Stacy & Bromm 2013;
- **KRO**, Kroupa 2001;
- **LAR**, Larson et al., 1998;
- **TOP**, Top-heavy, Liu-Bromm et al. 2020.

3 Mass ratios, *q*:

- **S12**, Sana et al. 2012;
- **Sorted** distribution;
- **SB13**, Stacy & Bromm 2013.

2 orbital periods, *P*:

- **S12**, Sana et al. 2012 **(SHORT)**;
- **SB13**, Stacy & Bromm 2013 **(LONG)**;

2 eccentricity distribution, *e*:

- **S12**, Sana et al. 2012;
- **Thermal** distribution, Kinugawa et al. 2014.

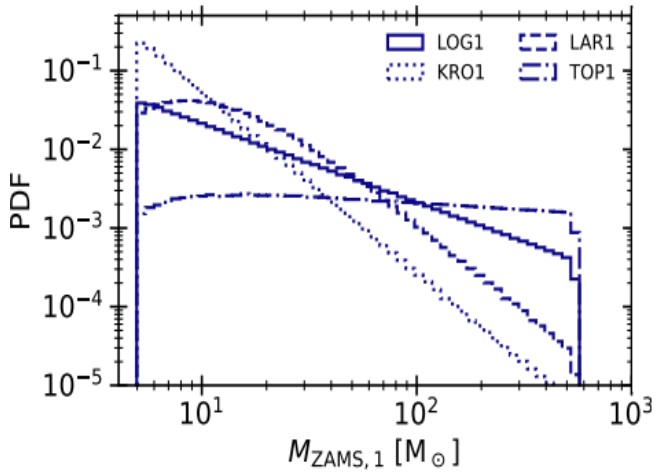

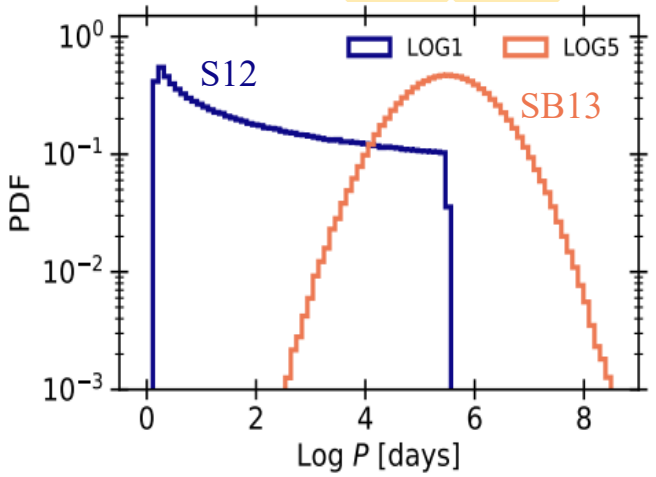

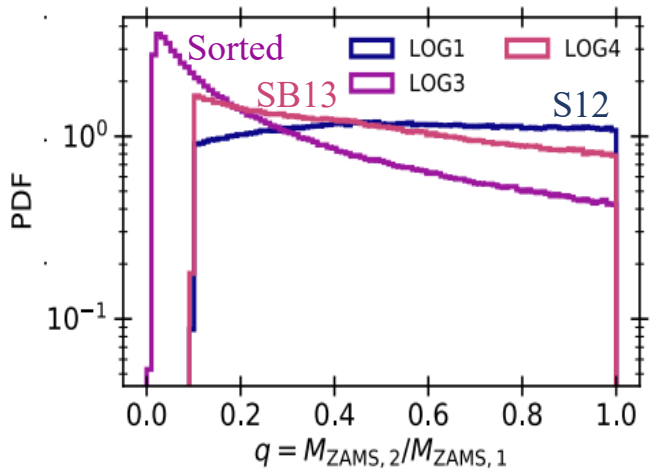

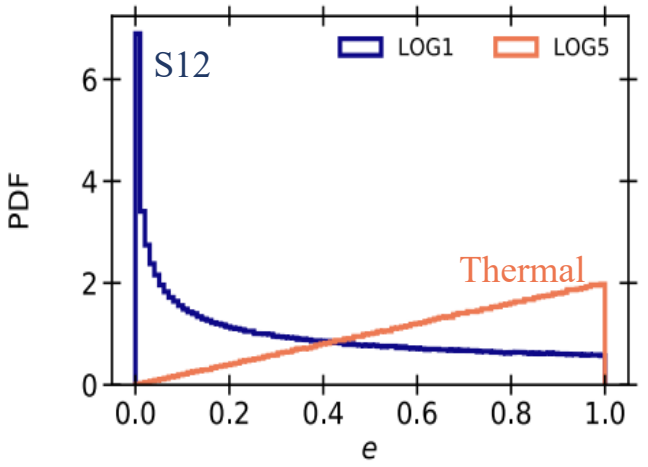

Population synthesis

Initial conditions

Model	$M_{\rm ZAMS,1}$	$M_{\rm ZAMS}$	Mass ratio q	Period P	Eccentricity e
LOG1	Flat in log	–	S12	S12	S12
LOG2	Flat in log	–	S12	SB13	Thermal
LOG3	–	Flat in log	Sorted	S12	S12
LOG4	Flat in log	–	SB13	S12	Thermal
LOG5	Flat in log	–	SB13	SB13	Thermal
KRO1	K01	–	S12	S12	S12
KRO5	K01	–	SB13	SB13	Thermal
LAR1	L98	–	S12	S12	S12
LAR5	L98	–	SB13	SB13	Thermal
TOP1	Top heavy	–	S12	S12	S12
TOP5	Top heavy	–	SB13	SB13	Thermal

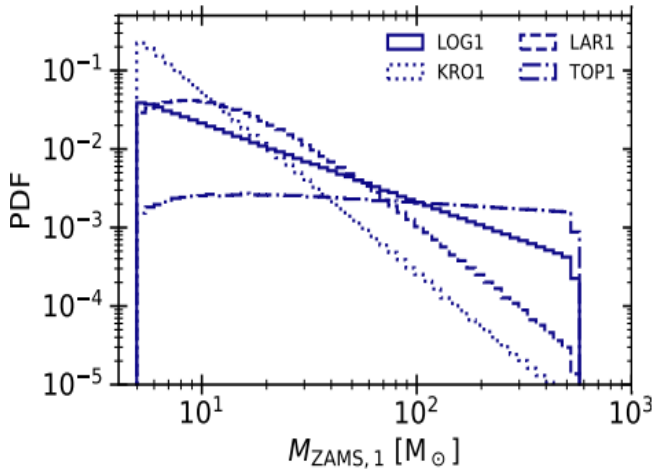

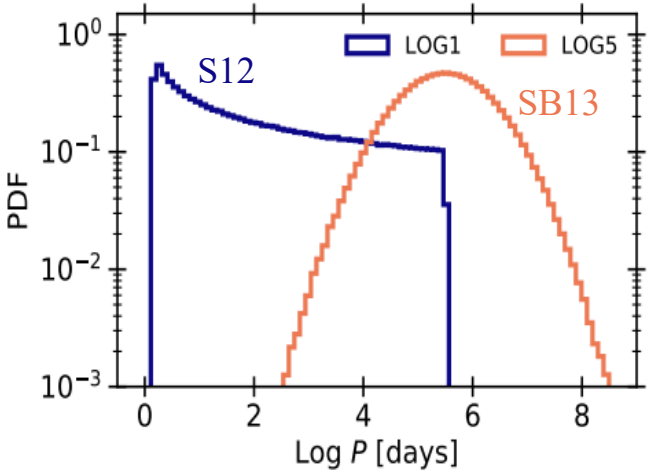

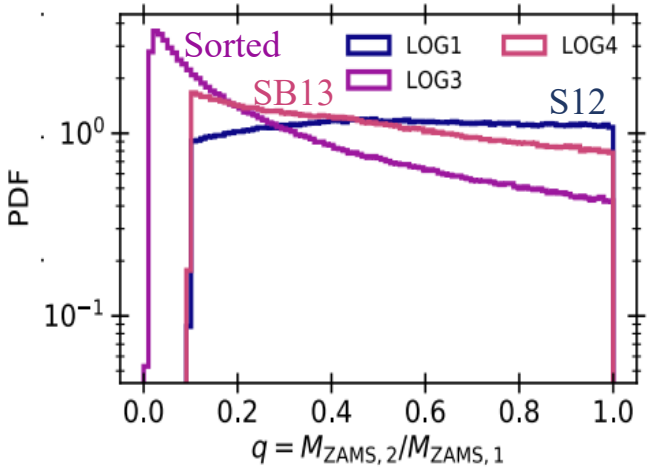

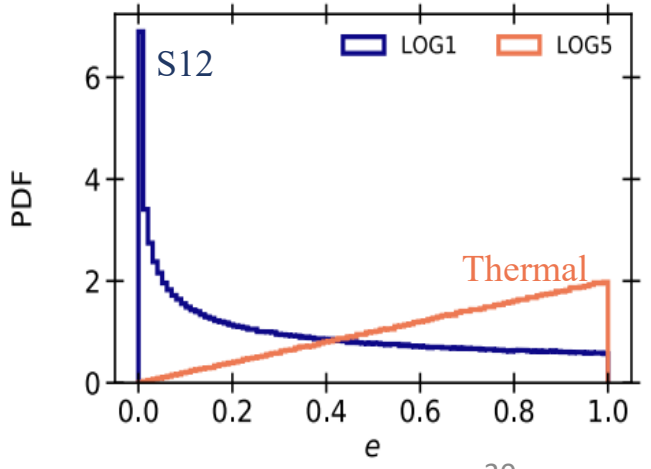

Population synthesis

Initial conditions

Model	$M_{\mathrm{ZAMS},1}$	M_{ZAMS}	Mass ratio q	Period P	Eccentricity e	N [$\times 10^7$]	Total mass [$\times 10^9$ $M_\odot$]
LOG1	Flat in log	–	S12	S12	S12	1.45	2.59
LOG2	Flat in log	–	S12	SB13	Thermal	1.45	2.58
LOG3	–	Flat in log	Sorted	S12	S12	1.38	3.19
LOG4	Flat in log	–	SB13	S12	Thermal	1.53	2.60
LOG5	Flat in log	–	SB13	SB13	Thermal	1.53	2.60
KRO1	K01	–	S12	S12	S12	5.23 (2.00†)	1.35 (0.89†)
KRO5	K01	–	SB13	SB13	Thermal	6.11 (2.00†)	1.52 (0.93†)
LAR1	L98	–	S12	S12	S12	2.00	1.20
LAR5	L98	–	SB13	SB13	Thermal	2.27 (2.00†)	1.30 (1.24†)
TOP1	Top heavy	–	S12	S12	S12	1.05	4.16
TOP5	Top heavy	–	SB13	SB13	Thermal	1.07	4.03

Population synthesis

Results

Configuration	Mass ratio	Period	Eccentricity
1	S12	S12	S12
5	SB13	SB13	Thermal

BBHs which merge within a Hubble time (~ 14 Gyr), BBHm

BBHm (%)	LOG1	LOG2	LOG3	LOG4	LOG5	KRO1	KRO5	LAR1	LAR5	TOP1	TOP5
Pop. III	11.25	0.75	9.33	11.57	0.68	14.66	0.85	14.34	0.91	6.47	0.36
Pop. II	13.53	0.97	10.88	14.46	0.86	16.23	1.15	16.15	1.16	8.52	0.48

The numbers of BBHs born from Pop. III stars are similar to those of BBHs born from Pop. II stars for all the considered models.

Population synthesis

Results

- In the case of Pop. II stars, equal-mass BBHs are the most common systems regardless of the model, even if models LOG5, KRO1, LAR5, and TOP5 show a mild secondary peak for q ~ 0.4 -- 0.5. In contrast, for Pop. III stars, the most common BBH mass ratio is 0.8 - 0.9 for the models LOG1, LOG3, LOG4, KRO1, LAR1, and TOP1, i.e. for all the models adopting the S12 initial period distribution. This is a consequence of the dominant evolutionary channels in such models.
- Finally, the distribution of delay times Cdel (i.e., the time elapsed between the formation of the binary system and the BBH merger) shows another difference between Pop. III and II BBHs (Fig. 11). All Pop. III models seem to match the trend tdel propto t-1 between 3 and 104 Myr. In contrast, some of the Pop. II models (LOG2, LOG5, KRO5, LAR5, and TOP5) show an excess of short delay times (3 -- 10 Myr). The models showing this excess share the SB13 orbital period distribution. This feature is another signature of the formation channel.

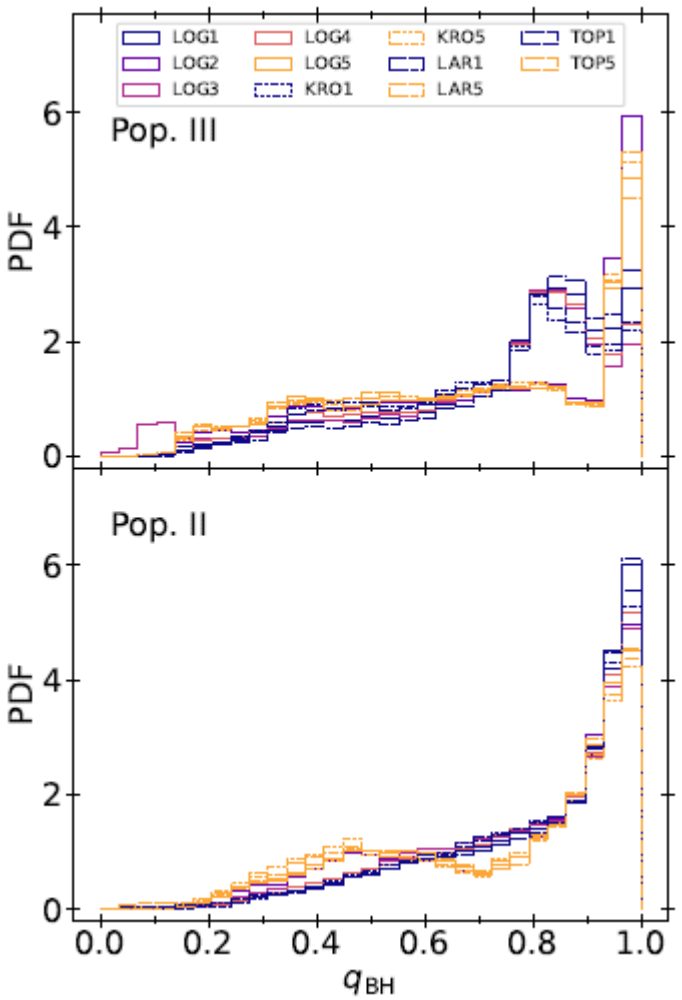

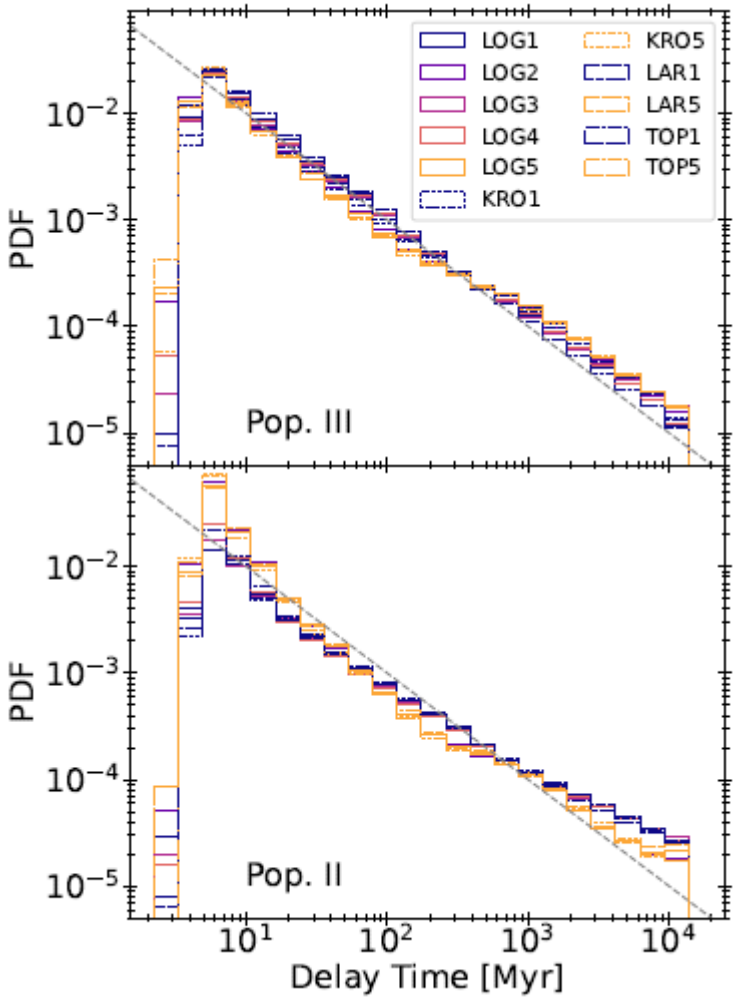

Population synthesis

Results

The masses distribution of Pop. III and Pop. II BBHms are similar.

- **A few BBHm with one component above the pair-instability mass gap.** Assuming that PI Mgap spans from 85 to 230 $M_{\odot}$, we find that BBH mergers with primary BH masses above the gap are up to 3.3 % (LOG3, Pop. III) and up to 0.09% (TOP5, Pop. II).
- **BBHm inside the gap are rare**. BBHms with primary BH mass inside the gap are up to 1.9% (LOG3, Pop. III) and up to 2.4% (TOP5, Pop. II).
- **Pop. II stars produce more BBHms with primary BH mass above the gap than Pop. III.**
- $\mathbf{M_s < 45\ M_{\odot}}$ for both Pop. II and III stars.

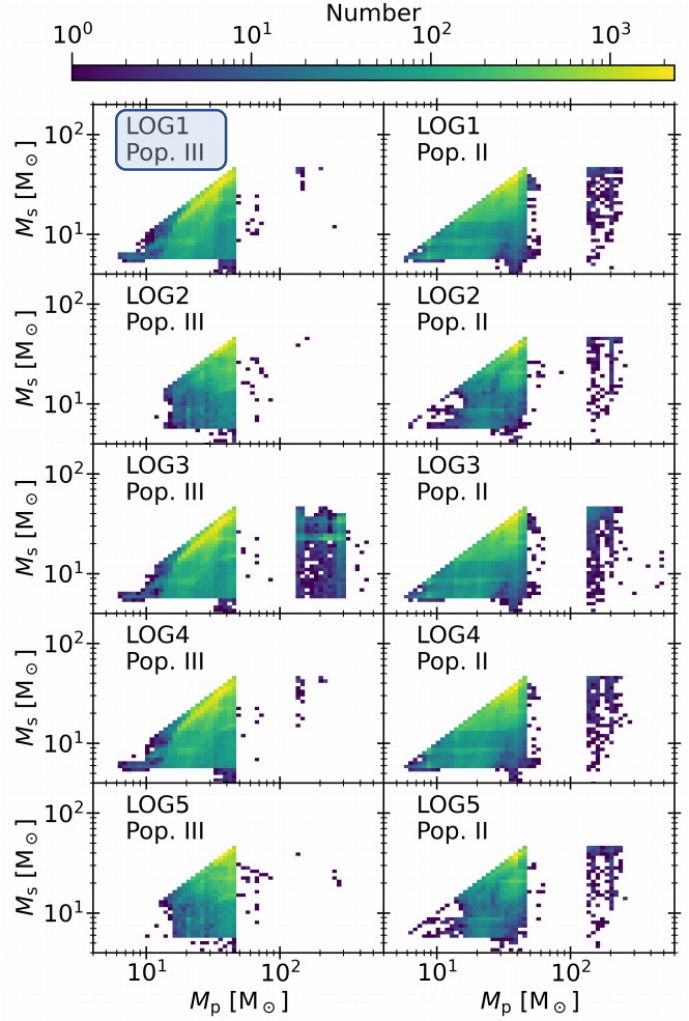

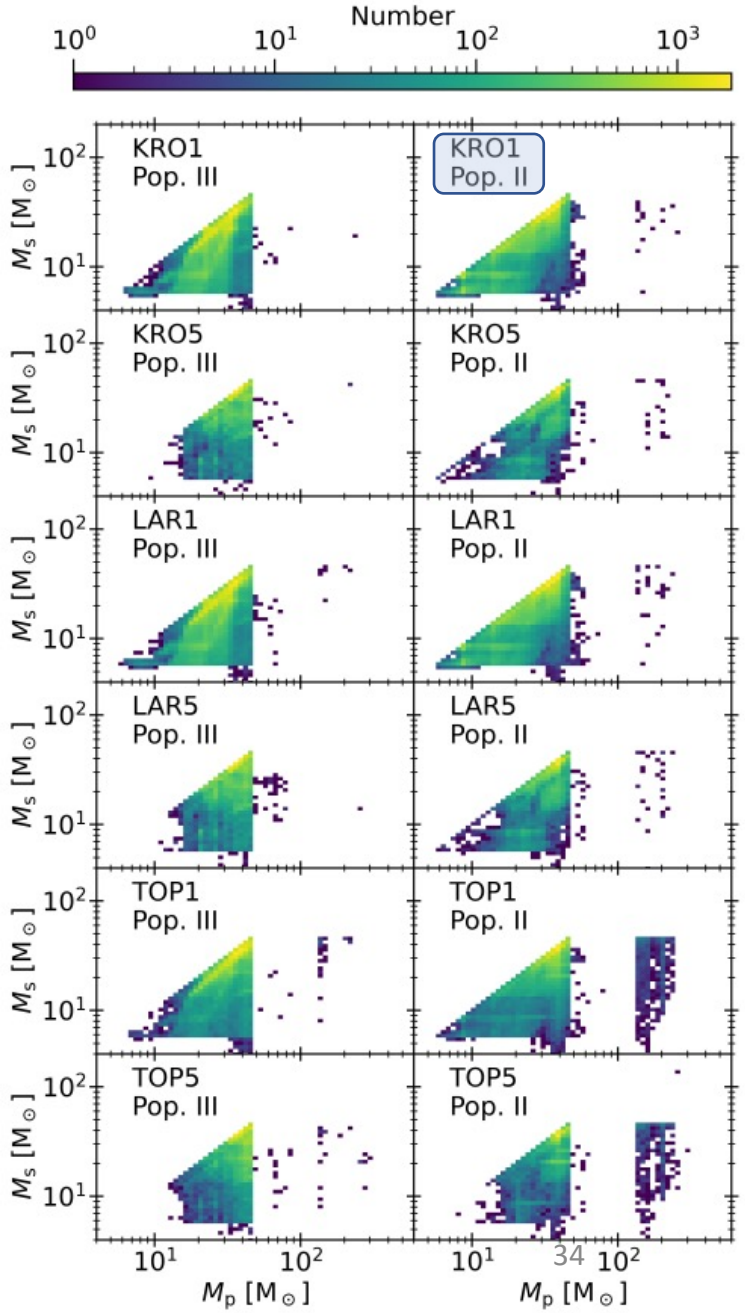

Population synthesis

Results

The masses distribution of Pop. III and Pop. II BBHms are similar.

- **Pop. II stars produce more BBHms with primary BH mass above the gap than Pop. III.**
- **A few BBHm with one component above the pair-instability mass gap.** Assuming that PI Mgap spans from 85 to 230 $M_{\odot}$, we find that BBH mergers with primary BH masses above the gap are up to 3.3 % (LOG3, Pop. III) and up to 0.09% (TOP5, Pop. II).
- **BBHm inside the gap are rare**. BBHms with primary BH mass inside the gap are up to 1.9% (LOG3, Pop. III) and up to 2.4% (TOP5, Pop. II).
- $\mathbf{M_s < 45\ M_\odot}$ for both Pop. II and III stars.

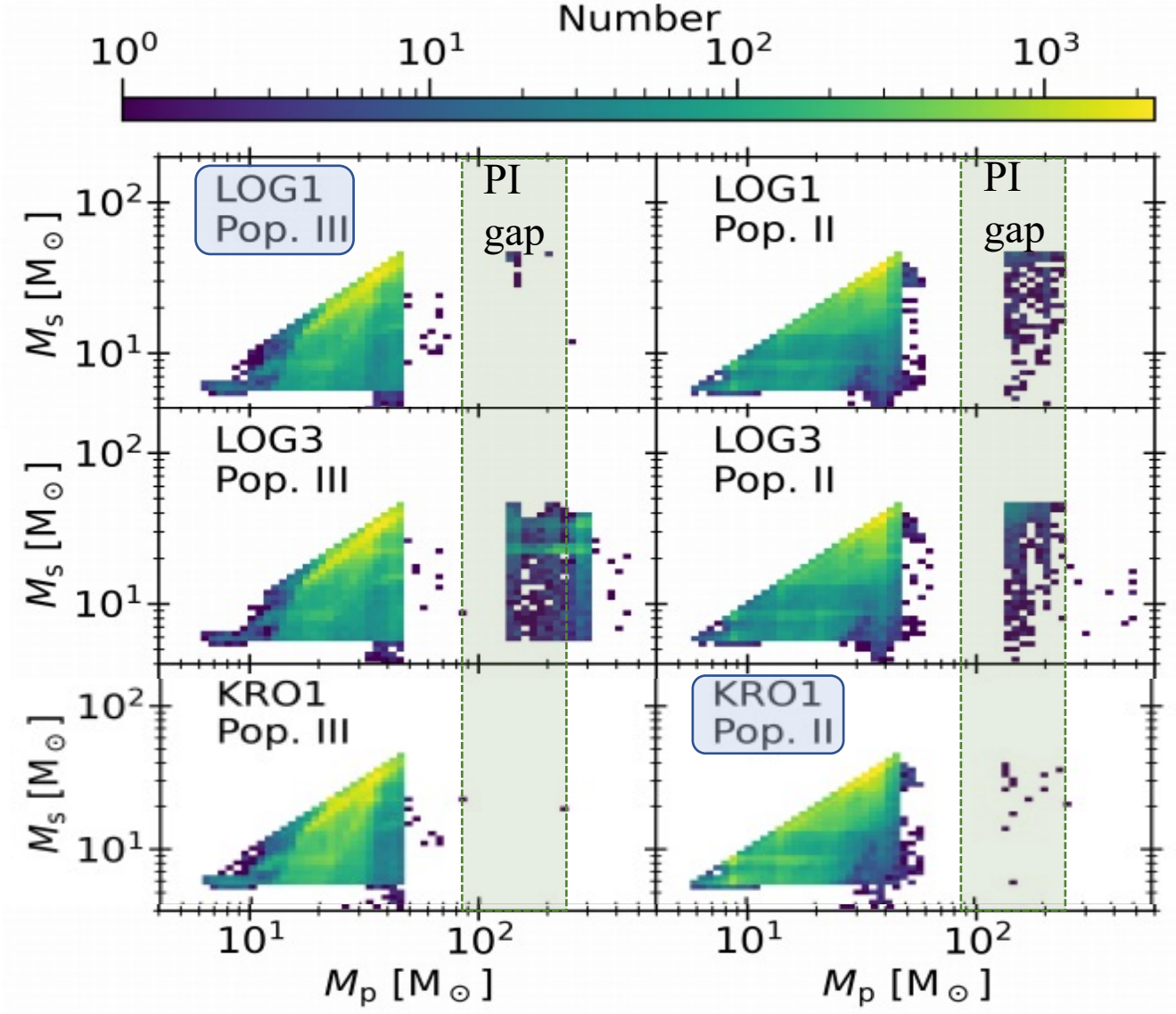

Population synthesis

Results – Formation channels

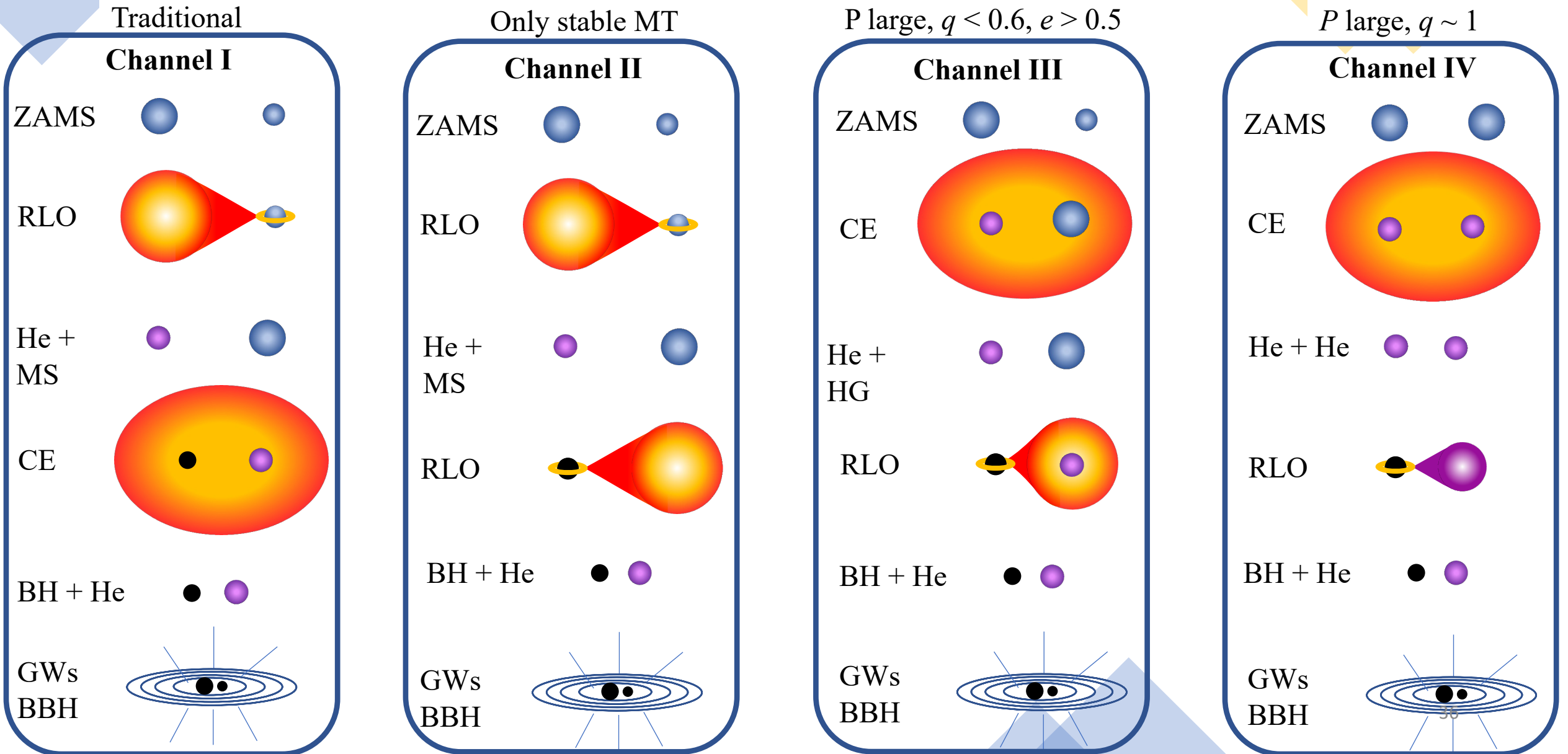

Population synthesis

Results – Formation channels

- **Channel 0:** very rare (<< 1%).
- **Channel I:** rare (< 7%).

- **Channel II** (stable mass transfer): dominant channel for models LOG1, LOG3, LOG4, KRO1, LAR1, and TOP1, for all the systems that adopt the initial S12 for the orbital periods (short).

  $q_{zams} \sim 0.5 - 0.9$, $q_{BH} \sim 0.75 - 0.9$.

- **Channels III and IV:** dominant channels for models LOG2, LOG5, KRO5, LAR5, and TOP5, models that adopt the SB13 orbital periods (large).

  - **Channel III:** $q_{BH} < 0.6$
  - **Channel IV:** $q_{BH} \sim 1$

Pop. I stars (Z = 0.002 – 0.01, from Iorio et al., 2022) show that between **50 and 80%** of all BBH mergers evolve via **channel I.**

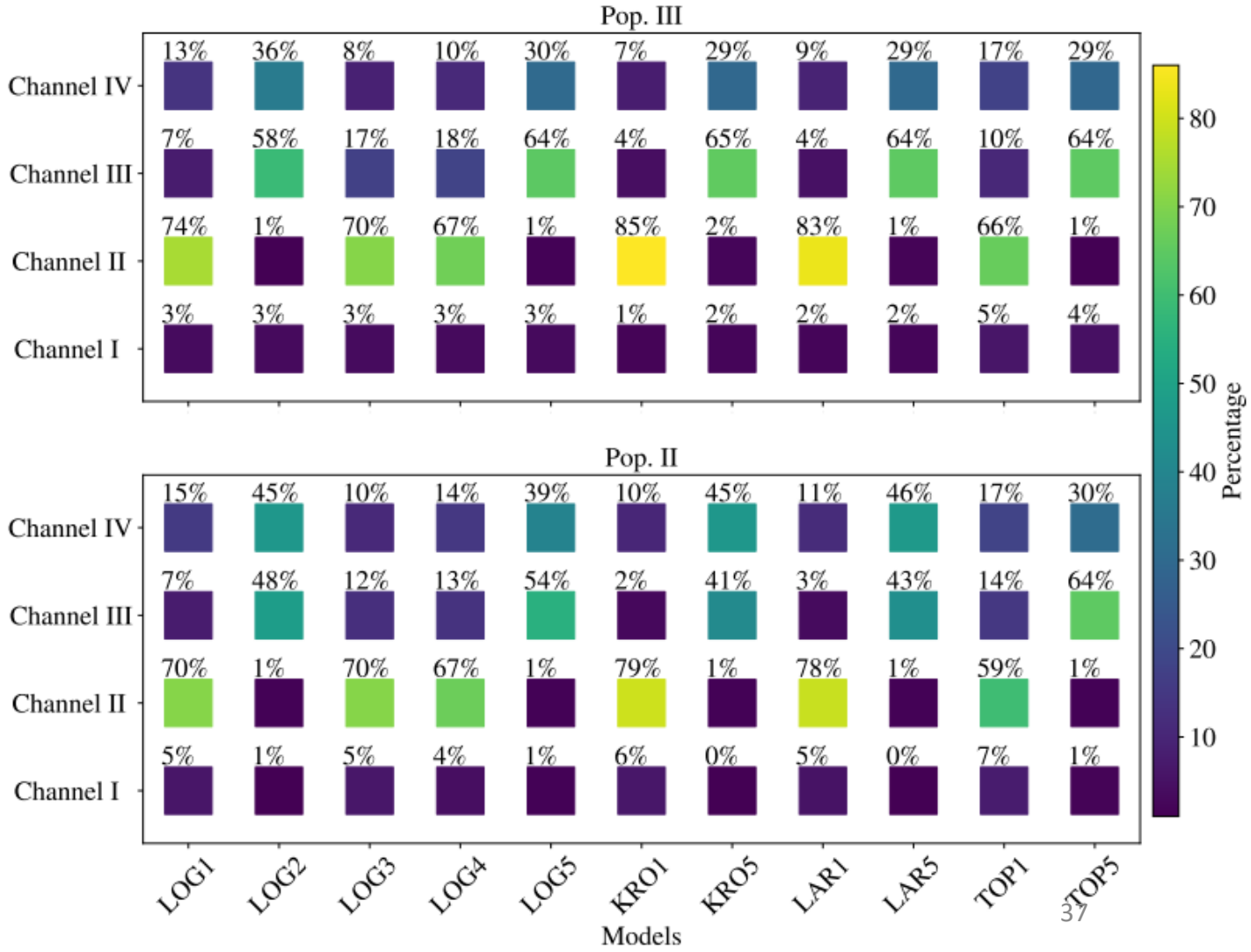

How confident are we of the PI mass gap edges?

Main uncertainties of stellar evolution:

- nuclear rates (Farmer+19, 20);
- fate of the envelope (mapelli+20);
- stellar convection (Costa+21);

^{12}C (α,γ) O^{16} rate +

Fate of H-rich envelope during the collapse

Lower edge mass gap

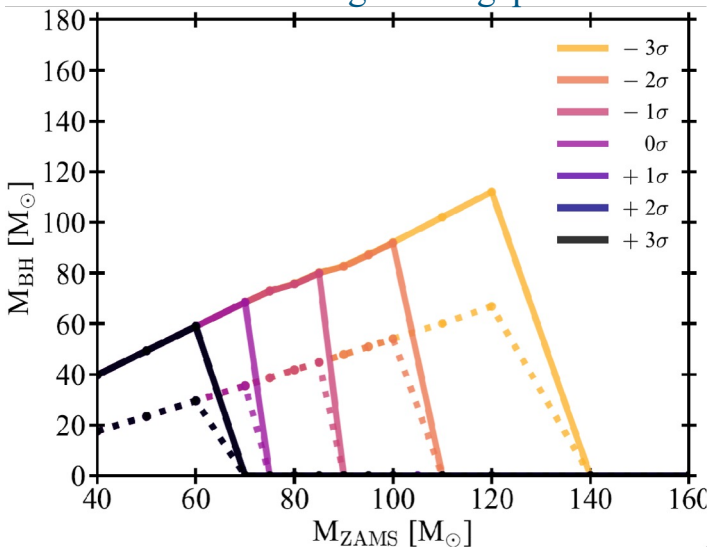

^{12}C (α,γ) O^{16} rate +

Fate of H-rich envelope during the collapse +

Envelope undershooting (i.e. convection)

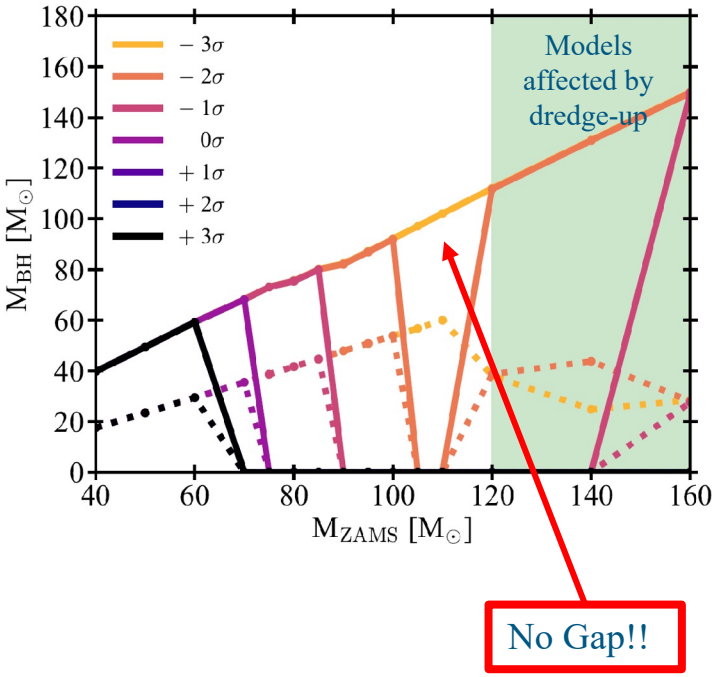

Effects of dredge-up

Two cases with 140 $M_\odot$

Without envelope undershooting

$\Lambda_{env} = 0$

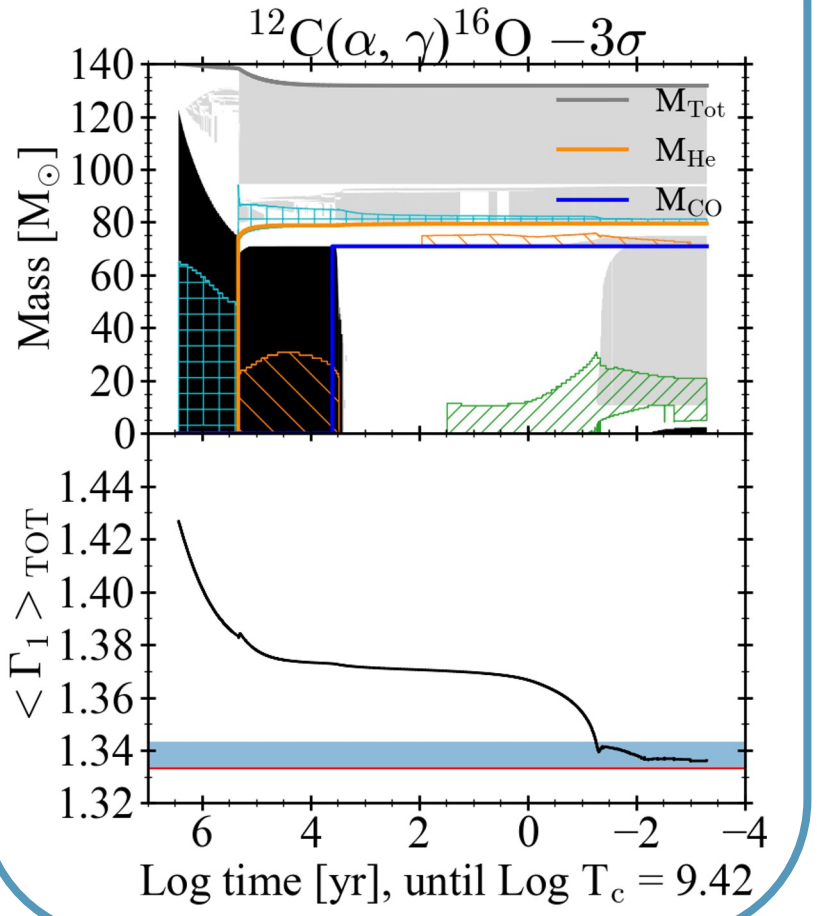

Dredge-up

With envelope undershooting

$\Lambda_{env} = 0.7\ H_P$

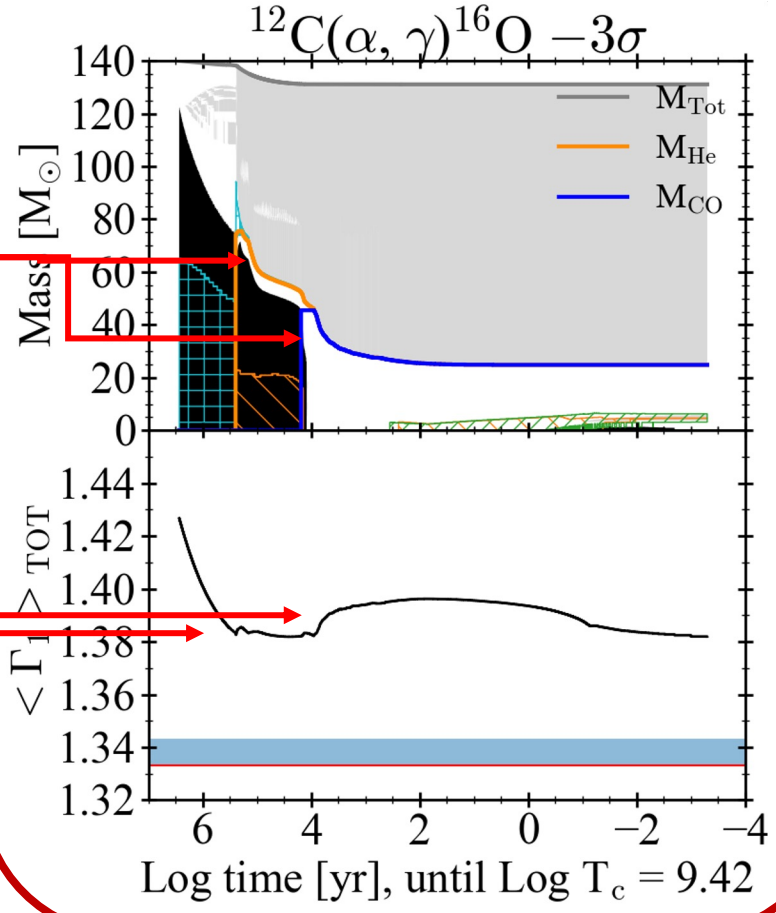

H-He shells interactions:

Chieffi & Limongi 2004, Ekstrom et al. 2008, Ritter et al. 2018, Clarkson & Herwig 2020, Farrell et al. 2021).

Effects of dredge-up

Dynamical stability criterion (Stothers, 1999)

$$\langle \Gamma_1 \rangle_{TOT} = \frac{\int_0^{M_*} \frac{\Gamma_1 P}{\rho} dm}{\int_0^{M_*} \frac{P}{\rho} dm} > \frac{4}{3} + 0.01$$

Γ_1 = first adiabatic exponent

Models with $M_{ZAMS} = 140\ M_\odot$

Without undershooting

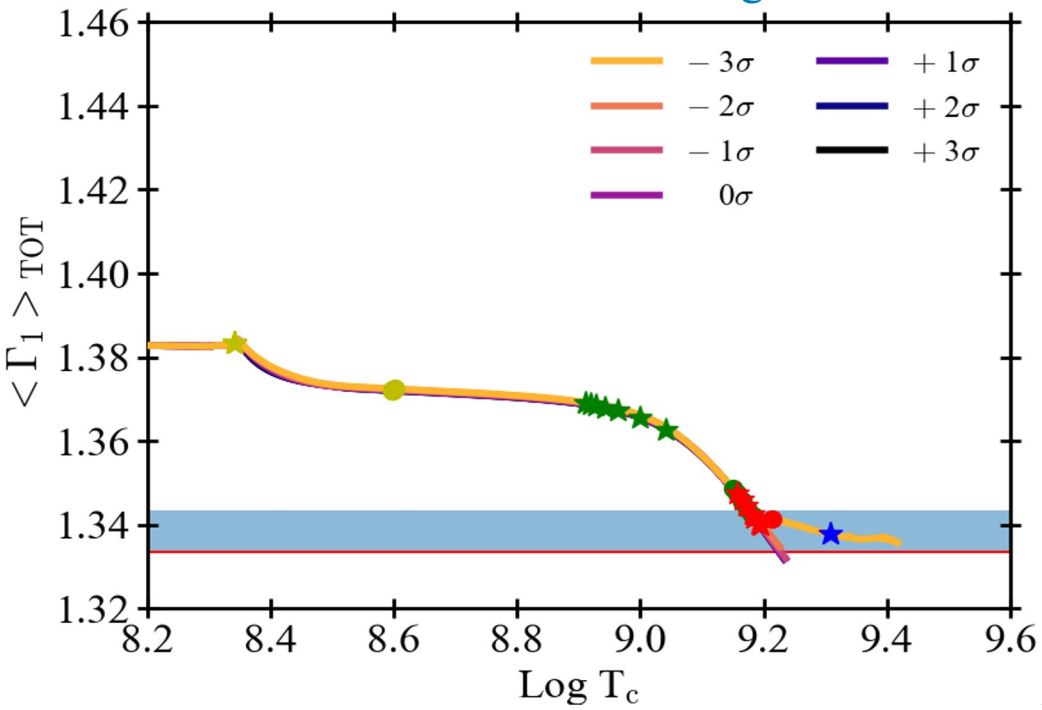

With undershooting

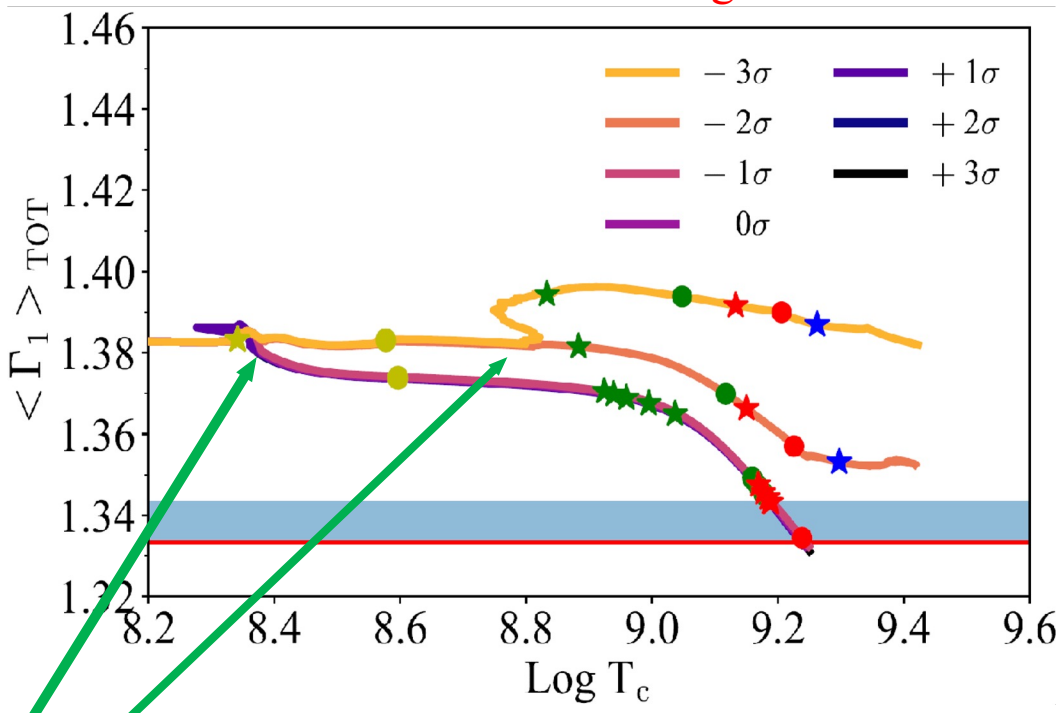

Dredge-up

In our binary simulations, it is even difficult to identify sharp edges for the pair-instability mass gap because of DUP episodes and mass transfer.